Final Report

Project Title: A Low-cost High-yield Process for the Direct Production of High Energy Density Liquid Fuel from Biomass
Award Number: DE-FG36-08GO18087

Recipient: Purdue University
Project Location: 480 Stadium Mall Drive, West Lafayette, IN 47907.

Reporting Period: June 1st, 2008 – May 31st, 2013
Date of Report: August 31st, 2013
Written by: R. Agrawal/ W.N. Delgass/ F. Ribeiro

> **IMPORTANT NOTE:** If any part of your quarterly report contains **proprietary/confidential information**, or details that should not be released to the general public, the specific sections of the report should be marked as such, by clearly marking the beginning and end of the confidential information. The marked sections will not be released to the general public or any unauthorized parties.

Status: Project Completed. Grant ended.

Executive Summary

The primary objective and outcome of this project was the development and validation of a novel, low-cost, high-pressure fast-hydropyrolysis/hydrodeoxygenation (HDO) process (H_2Bioil) using supplementary hydrogen (H_2) to produce liquid hydrocarbons from biomass. The research efforts under the various tasks of the project have culminated in the first experimental demonstration of the H2Bioil process, producing 100% deoxygenated >C4+ hydrocarbons containing 36-40% of the carbon in the feed of pyrolysis products from biomass. The demonstrated H_2Bioil process technology (i.e. reactor, catalyst, and downstream product recovery) is scalable to a commercial level and is estimated to be economically competitive for the cases when supplementary H_2 is sourced from coal, natural gas, or nuclear. Additionally, energy systems modeling has revealed several process integration options based on the H_2Bioil process for energy and carbon efficient liquid fuel production.

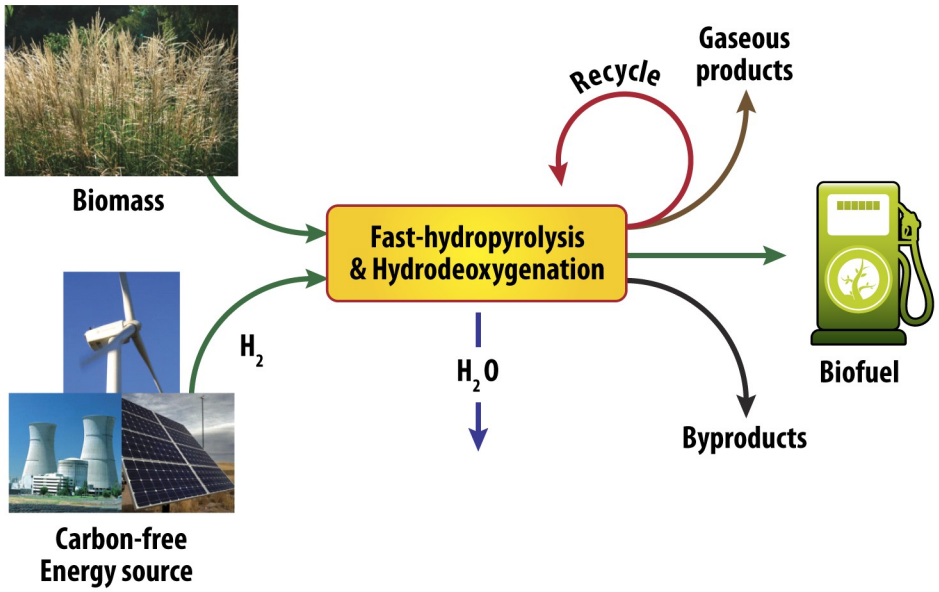

Figure 1. H_2Bioil Process using a novel fast-hydropyrolysis/ hydrodeoxygenation reactor.

All project tasks and milestones were completed or exceeded. Novel, commercially-scalable, high-pressure reactors for both fast-hydropyrolysis and hydrodeoxygenation were constructed, completing Task A. These reactors were capable of operation under a wide-range of conditions; enabling process studies that lead to identification of optimum process conditions. Model compounds representing biomass pyrolysis products were studied, completing Task B. These studies were critical in identifying and developing HDO catalysts to target specific oxygen functional groups. These process and model compound catalyst studies enabled identification of catalysts that achieved 100% deoxygenation of the real biomass feedstock, sorghum, to form

hydrocarbons in high yields as part of Task C. The work completed during this grant has identified and validated the novel and commercially scalable H_2Bioil process for production of hydrocarbon fuels from biomass. Studies on model compounds as well as real biomass feedstocks were utilized to identify optimized process conditions and selective HDO catalyst for high yield production of hydrocarbons from biomass.

In addition to these experimental efforts, in Tasks D and E, we have developed a mathematical optimization framework to identify carbon and energy efficient biomass-to-liquid fuel process designs that integrate the use of different primary energy sources along with biomass (e.g. solar, coal or natural gas) for liquid fuel production. Using this tool, we have identified augmented biomass-to-liquid fuel configurations based on the fast-hydropyrolysis/HDO pathway, which was experimentally studied in this project. The computational approach used for screening alternative process configurations represents a unique contribution to the field of biomass processing for liquid fuel production.

Task number: [A] Construction of Experimental Set-up

High-Pressure, Continuous-Flow Fast-hydropyrolysis Reactor

A significant effort was undertaken, as part of this grant, to design a high-pressure biomass feeder and a high-pressure continuous-flow fast-hydropyrolysis reactor that performs reliably, fits into the walk-in hood space in our laboratory, and has safety features for use of high-pressure hydrogen. One of the goals of the project was to identify optimum operating conditions for high-pressure biomass fast hydropyrolysis, as no systematic information, to our knowledge, exists in the literature on this subject. For the overall process to succeed, the optimum operating conditions were first identified and then the high pressure reactors and process were designed and developed. We believe that we were successful in identifying the optimal operating window at the lab scale and then designing a fast-hydropyrolysis and catalytic hydrodeoxygenation reactor system to demonstrate the process.

It is challenging to feed solids under high pressure at the lab scale. For the fast-hydropyrolysis reactor, we designed a unique feeder system to feed biomass at 0.1 - 20 g min^{-1} and tested it up to 68 bar pressure, which achieved A.ML.1 grant milestone (completion of high pressure screw feeder with a minimum operating pressure of 1000psig). To our knowledge, no other academic system exists that can perform such a study. On the large scale, high pressure operation is widespread in the petroleum refining industry. High pressure solid feeders are also used for coal gasification and in the paper industry. But, we note that a lab-scale continuous-flow high-pressure solids feeder was not commercially available for the flow rates suitable for lab scale operation, hence we overcame a significant challenge of designing and building it in-house.

For the fast-hydropyrolysis reactor, over six different prototype designs were tested under inert atmosphere at moderate pressure (300-500 psig) with varying reactor geometries. Nearly all of the problems in the preliminary designs stemmed from clogging at the biomass inlet to the reactor. For example, it was determined that below a critical gas velocity, solids would accumulate near the reactor entrance and slowly pyrolyze, forming char and eventually clogging the entrance. Additionally, more traditional designs such as free-fall and bubbling fluidized-bed reactors could not be used due to vertical space constraints or limitations in hydrogen flow rates imposed for safety reasons. In FY10-Q4 we completed a series of experiments on a prototype, cyclone-type, high-pressure, fast-pyrolysis reactor and found it to be best suited to our laboratory space constraints and reliable under typical operating conditions with cellulose as a model feedstock. We used the results from these prototype experiments to design a second-generation cyclone-type fast-hydropyrolysis reactor with optimized geometry and pressure vessel ratings that met the requirements for working at high pressures and temperatures. The heating rates in this fast-hydropyrolysis reactor are >300 °C/s based on heat transfer calculations and the vapor residence time in the reactor is on the order of 2 seconds. This fast-hydropyrolysis reactor was coupled with a vapor-phase catalytic fixed-bed hydrodeoxygenation (HDO) reactor. The complete reactor system is shown in Figure 1. Table 1 shows the operating ranges of this reactor

system. Both reactors are capable of being operated at high hydrogen partial pressures (up to 100 bar) and high temperatures up to 650 °C. Associated laboratory safety systems and procedures for usage of high-pressure hydrogen were also developed, in addition to process control systems for the fast-hydropyrolysis reactor. After finishing construction of the reactor, safety and control systems, shakedown experiments in high-pressure inert atmosphere (fast-pyrolysis) to refine standard operating procedures for use with hydrogen and debug the equipment and process control systems were completed. With these experiments, we achieved reactor performance milestone A.ML.2 (minimum of 70% conversion to liquid and gases from model compound (cellulose) fast-pyrolysis) in the lab scale cyclone reactor. This reactor system has also been used to complete work on other specific tasks and milestones, as explained in subsequent sections.

Figure 1. Completed high-pressure, cyclone-type, fast-hydropyrolysis reactor.

Table 1. High-pressure, continuous-flow, fast-hydropyrolysis reactor system design ranges.

Biomass and Gas Flow rate Ranges	
Biomass Feed rate	0.1-5 g min^{-1}
He/N_2/H_2/CO flow rate (each)	1-50 SLPM
Maximum design pressure	100 bar
Fast-hydropyrolysis reactor	
Max. Temperatures : Wall/ top flange/ bottom flange	650 °C / 650 °C / 590 °C
Fixed-bed, catalytic HDO reactor and connector	
Max. Temperatures: Wall / Flange	650 °C / 593 °C

Micro-batch, Fast-hydropyrolysis Reactor

The micro-batch fast-hydropyrolysis reactor (pyroprobe) is a commercially available unit (Pyroprobe 5200, CDS Analytical, Oxford, PA). A resistively-heated platinum coil is utilized to heat biomass samples at a maximum possible heating rate of 20,000 °C s^{-1}. A quartz tube was used to hold the biomass sample, which was heated externally by the Pt coil. The vapor products of pyrolysis are carried out of the pyrolysis zone by the flowing H_2 gas without coming in contact with the heated Pt coil. A basic schematic of the pyroprobe reactor system is shown in Figure 2 and Figure 3. The Pt coil which houses the sample quartz tube is inserted into the temperature controlled zone which can be pressurized up to 34 bar with He/H_2. The products of pyrolysis are analyzed via a GC/MS. The GC/MS system (Agilent 7890GC and 5975MS) uses a mid-polarity (DB1701) column for the chromatographic separation of products, while the quantification is achieved via a flame ionization detector (FID). A fixed-bed catalytic reactor for hydrodeoxygenation (HDO) of pyrolysis products is located downstream of the pyrolysis region between the pyroprobe and valve box (Figure 3).

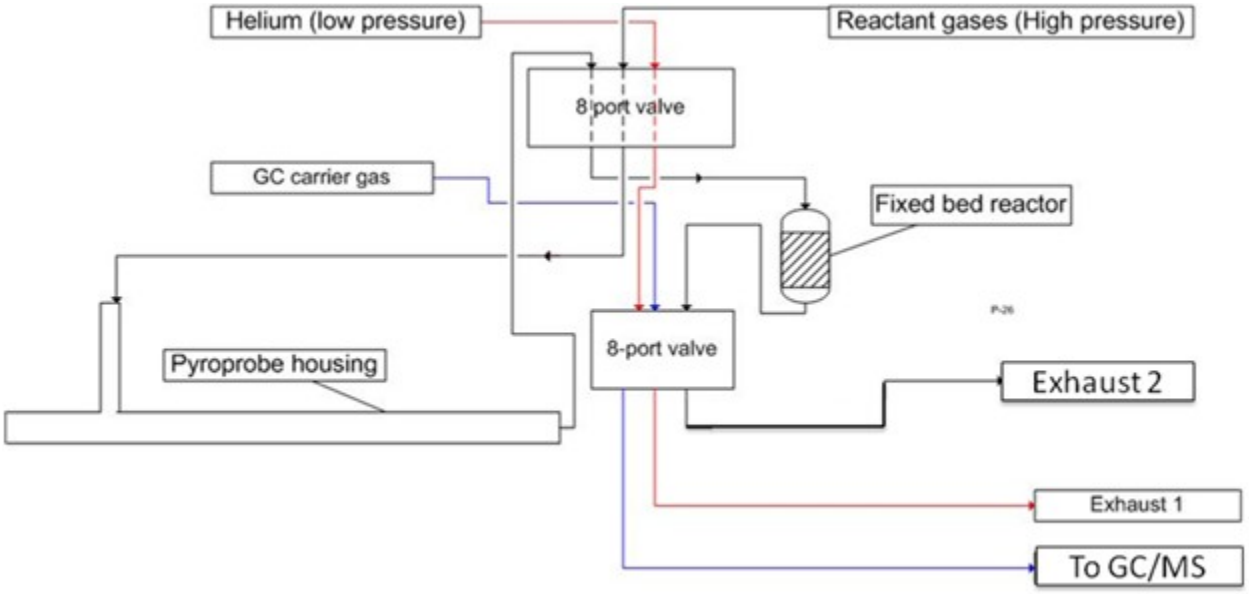

Figure 2. Schematic of the micro-batch fast-hydropyrolysis reactor and fixed-bed catalytic reactor arrangement during loading phase.

The sample loading for biomass or model compounds for a single experiment is in the range of 100-1000 µg. Operation of the pyroprobe occurs in to two phases – the loading phase and the reactor operation phase. The loading phase is used to load the sample into the pyroprobe housing. During the loading phase of the experiment, the fixed bed reactor is isolated from the pyroprobe housing by means of two 8-port valves (Figure 2), which prevents the catalyst from being exposed to air. After loading the sample into the pyroprobe housing, low pressure helium gas flow is used to flush out air from the system. The 8-port valves are switched during reactor operation phase (Figure 3) and allow the reactant gas to flush out the helium gas from the pyroprobe housing. The

probe is then heated in a controlled manner and the pyrolysis vapors are carried through the fixed bed reactor to the GC/MS for analysis.

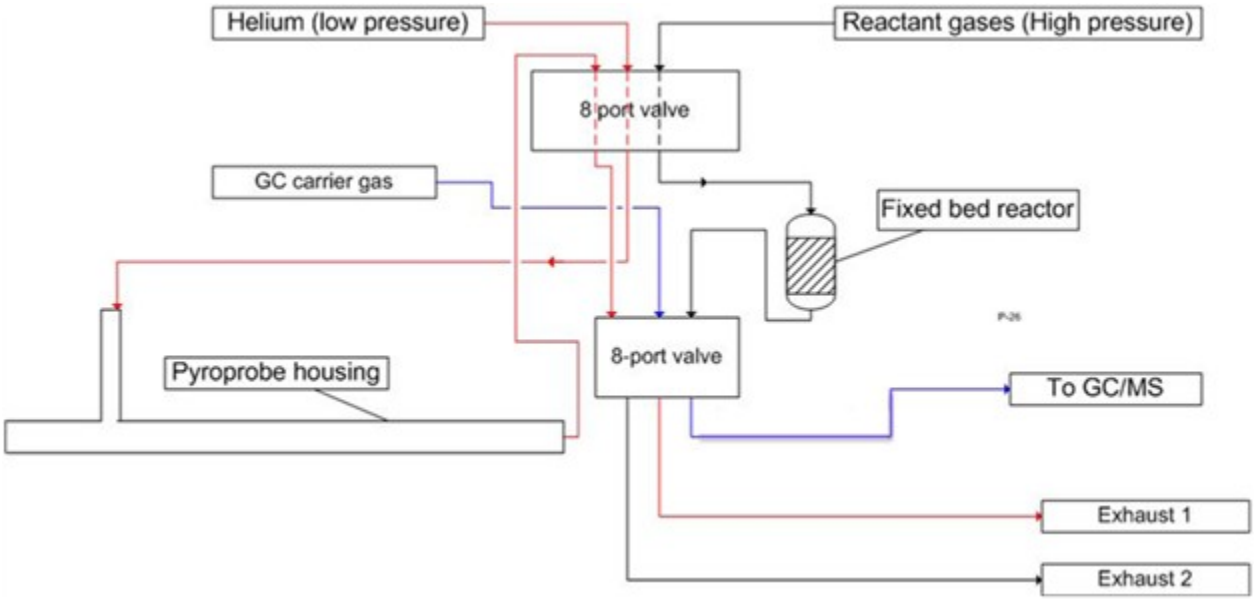

Figure 3. Schematic of the micro-batch fast-hydropyrolysis reactor and fixed-bed catalytic reactor arrangement during reactor operation.

Standalone Secondary HDO Reactor for Model Compound Studies

In addition to the high-pressure continuous-flow fast-hydropyrolysis/HDO reactor, a secondary high-pressure hydrodeoxygenation (HDO) reactor was designed and constructed to allow for isolated studies of the second stage HDO reactions and for catalyst development. The reactor system is composed of a vapor-phase, fixed-bed, plug-flow, catalytic reactor capable of operation up to 1000psi in He/H_2 environments and temperatures >500°C, although typical operation is at 300°C. In FY10-Q3 initial experiments were conducted on the catalytic HDO of lignin model compounds at atmospheric pressure. As the results from these low pressure studies did not show desirable HDO activity, in FY-10-Q4 and FY11-Q1, the standalone secondary high-pressure hydrodeoxygenation (HDO) reactor was modified to allow for high pressure operation up to 1000psi in an inert or pure hydrogen environment. Modification of the reactor system for high-pressure included installation of a high-pressure ISCO syringe pump for liquid model compound feed introduction, and design of high-pressure and hydrogen safety and control systems.

All gas and vapor phase products are analyzed with an online Agilent 6890N gas chromatograph with a Carboxen-1000 column connected to a thermal conductivity detector and a SPB-1 capillary column connected to a Agilent Deans Switch 3-way splitter which splits the flow to a Flame Ionization Detector and a Agilent 5973N Mass Spectrometer. Mass balances close to 100% ± 5%.

Overall, we have designed and safely operated high-pressure reactors that will fulfill the challenging and demanding conditions needed for fast-hydropyrolysis/HDO. These include: 1) rapid heating rates >300^{o}C/s, 2) high hydrogen partial pressures to minimize catalyst coking and improve selectivity to fully deoxygenated products, and 3) high temperatures > 500^{o}C.

Task number: [B] Model Compounds Study

In this section, we would like to point out that all grant tasks and milestones related to model compound fast-hydropyrolysis and hydrodeoxygenation catalysts testing have been completed. Model compounds are useful to deconvolute the effects of process conditions, chemical pathways, and develop catalysts to target specific oxygen functional groups, which would not be possible using a mixture of compounds from real biomass fast-hydropyrolysis. These experimental results from model compounds have been documented in the various quarterly reports associated with the grant. For instance, we achieved several practical reactor performance milestones such as milestone A.ML.2 (70% liquid bio-oil yield from model compound fast-hydropyrolysis) in the lab scale cyclone reactor. We also achieved milestone B.ML.1 (35 wt% reduction in oxygen in a model bio-oil compound with at least 20wt% oxygen) in the standalone secondary HDO model compound reactor via hydrodeoxygenation (HDO) of a lignin model compound. In addition to this, we performed fast-hydropyrolysis (FHP) on cellulose followed by hydrodeoxygenation with candidate catalysts (mainly identified from model compounds study as part of Tasks B.3) on cellulose FHP vapors which achieved 100% deoxygenation to produce fully deoxygenated hydrocarbons in both the lab-scale and micro-scale reactor, which achieved and exceeded the oxygen reduction milestone B.ML.2 (35 wt% reduction of oxygen in oil made from a model biomass compound using high-pressure fast-hydropyrolysis with or without a HDO catalyst as compared to conventional pyrolysis in inert atmosphere). Our contributions to meeting deoxygenation targets, and in particular reaching 100% feed deoxygenation on the lab-scale and micro-scale reactor are inherently very important milestones that took years of testing complicated high-pressure reactor designs, analytical developments, and catalyst development to achieve.

[B.1] Model Compounds Study - Conventional fast-pyrolysis and fast-hydropyrolysis in a single stage

High-Pressure, Continuous-Flow Fast-hydropyrolysis Reactor

In FY11-Q2, initial shakedown experiments were completed on the high-pressure fast-hydropyrolysis reactor. Initial experiments were completed in a high-pressure (25 bar and 50 bar) inert atmosphere, with cellulose as model feedstock, to get experience working with the reactor and to refine equipment design and safety related operating procedures for the reactor. In FY11-Q3, conventional fast-pyrolysis and fast-hydropyrolysis in a single stage on a biomass model compound (Task B.1), was completed. The fast-pyrolysis and fast-hydropyrolysis experiments were conducted using cellulose as a model biomass feedstock, at 25 bar inert partial pressure or 25 bar hydrogen partial pressure respectively. The pyrolysis temperature and the total gas flow rates (at standard conditions) were kept constant for comparison between the experiments, to understand the effect of high-pressure hydrogen on the pyrolysis products. These experiments completed Task B.1. The fast-hydropyrolysis experiments provided a baseline for comparison with experiments using candidate HDO catalysts in

the on-stream fixed-bed catalytic reactor downstream of the fast-hydropyrolysis reactor (Task B.2).

Experimental Methods

All the experiments were carried out on the high-pressure, cyclone-type, fast-hydropyrolysis reactor system (Figure 1). The feedstock for these experiments was microcrystalline cellulose with mean particle size 50 μm (Sigmacell cellulose, Type 50). After pyrolysis, the vapor products passed through a connector section and an empty HDO reactor section with no HDO catalyst. The pyrolysis vapors then moved through a concentric tube condenser, which cooled the vapors to below room temperature, and a trap cooled by a mixture of ice and water. Condensed vapors were separated from permanent gases by a coalescing filter and the liquid products were collected in the traps. A sample of the exhaust gases was analyzed with a gas chromatograph (GC) with a thermal conductivity detector (TCD) to measure the composition of CO, CO_2, H_2 and CH_4 in the permanent gas products (using nitrogen internal standard). The collected liquid products (organics + water) were analyzed by elemental analysis to determine C/H/O content and Karl Fischer titration to determine the water content. Both analyses were used to evaluate the liquid product oxygen content (on a dry basis) and the percentage weight reduction in the oxygen content in the liquid product as compared to the feed cellulose.

For understanding the relative effect of hydrogen pressure on the pyrolysis liquid product composition, the collected liquid products from the comparative fast-pyrolysis and fast-hydropyrolysis (without HDO catalyst) experiments were analyzed by atmospheric-pressure, chemical-ionization, mass spectrometry (APCI-MS) method. A specially developed method for ionization, using chloride ion addition, was used for analysis to avoid fragmentation of product molecules. This technique is semi-quantitative and allows for comparisons of relative abundances of the species present in the liquid products.

Results and Discussion

In FY11-Q3, conventional fast-pyrolysis and fast-hydropyrolysis in a single stage on a biomass model compound (Task B.1), was completed. The experimental summary for these comparative experiments is shown in Table 2. The cellulose fast-hydropyrolysis experiment was conducted at 25 bar hydrogen partial pressure and the comparative cellulose fast-pyrolysis experiment was conducted at 25 bar helium partial pressure. The average pyrolysis temperature was ~480^{o}C for both the experiments.

The overall mass balances for the experiments are shown in Table 3. There were no significant differences in the product distributions (yields of liquid, char and gases) of the two experiments. The overall mass balances were closed to within 15-20% for both the experiments. Error in the overall mass balance can be accounted by, for example, 1) errors in the gas phase measurement due to a slow GC sampling rate of the permanent gas stream, which only allowed two/three samples during the run and therefore

prevented proper integration of gas production over time and 2) errors due to the solvent flushing procedures to remove system holdup of liquids and solids.

Table 2. Experimental summary for fast-hydropyrolysis and fast-pyrolysis experiments with 50 µm cellulose feedstock. (No HDO catalyst)

	Fast-hydropyrolysis	*Fast-pyrolysis*
Feedstock	50 µm cellulose	50 µm cellulose
Feed rate / g min^{-1}	0.9	0.9
Total mass fed / g	40.7	56.4
Hydrogen flow rate / (std) L min^{-1}	34.7	0
Helium flow rate / (std) L min^{-1}	0	34.7
Nitrogen flow rate / (std) L min^{-1}	3.0	3.0
Total pressure / bar	27	27
Hydrogen partial pressure / bar	25	0
Helium partial pressure / bar	0	25
Average pyrolysis temperature / °C	~480	~480
Vapor residence time in reactor / s	2.4	2.3

Table 3. Overall mass balance for fast-hydropyrolysis and fast-pyrolysis experiments with 50 µm cellulose feedstock.

	Fast-hydropyrolysis	*Fast-pyrolysis*
Liquid yield / wt %	66.9	69.2
Char yield / wt %	8.3	7.7
Gas yield / wt %	5.5	7.6
CO / wt %	2.1	3.3
CO_2 / wt %	3.2	4.1
CH_4 / wt %	0.2	0.2
Overall mass balance / %	80.7	84.6

APCI-MS with chloride ion attachment was utilized to identify the presence of major species in the liquid products produced from the fast-pyrolysis and fast-hydropyrolysis of cellulose in both runs. Figure 4 shows a comparison of the mass spectra of the liquid products of the two experiments in the high mass range (50 to 1000 Da). Comparison of the mass spectra shows no significant differences in the types of product molecules from fast-hydropyrolysis and fast-pyrolysis of cellulose at these process conditions. The most abundant peaks correspond to the chloride adduct of a dehydrated glucose building block monomer ($C_6H_{10}O_5Cl$; 197 Da), followed by the chloride adduct of one cellulose dimer ($C_{12}H_{20}O_{10}Cl$; 359 Da). The challenge will be to deoxygenate the molecules in these liquid products to enhance their energy density while minimizing breakage of the molecule into smaller fragments. These results from Task B.1 suggest that the role of a HDO catalyst will be very important for hydrogen to participate in deoxygenation and have an effect on the pyrolysis products (Tasks B.2).

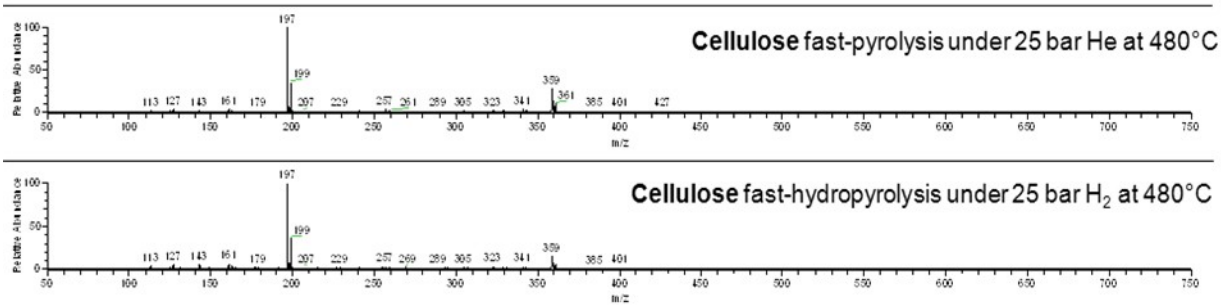

Figure 4. Comparison of APCI-MS spectrums of liquid products produced in cellulose fast-pyrolysis and fast-hydropyrolysis at 480°C. The spectrum shows the relative abundance of masses (m/z) 50 Da to 1000 Da.

The C/H/O (on wet and dry basis) and water content of the liquid products from both the experiments are shown in Table 4. On a dry basis, the composition of the liquid products from both the experiments were comparable, within experimental error. The presence of high-pressure hydrogen (with no HDO catalyst) resulted in no appreciable deoxygenation of the fast-hydropyrolysis vapors. This fast-hydropyrolysis experiment was used as a baseline comparison for deoxygenation in the presence of candidate HDO catalysts in a high-pressure hydrogen environment (Task B.2).

Table 4. Elemental analysis of liquid products produced from the fast-pyrolysis and fast-hydropyrolysis of cellulose at 480 C.

	Fast-hydropyrolysis	*Fast-pyrolysis*
Carbon (wet basis) / wt %	39.81	38.97
Hydrogen (wet basis) / wt %	7.45	7.51
Oxygen (wet basis) by difference / wt %	52.74	53.51
Water content / wt %	18.47	21.51
Carbon (dry basis) / wt %	48.82	49.65
Hydrogen (dry basis) / wt %	6.62	6.52
Oxygen (dry basis) by difference / wt %	44.56	43.83
Empirical formula (dry basis)	$CH_{1.616}O_{0.685}$	$CH_{1.567}O_{0.663}$

In summary**,** after incremental improvements to reactor design and safety reviews based on initial shakedown experiments, Task B.1 was completed by performing fast-hydropyrolysis experiments of cellulose at 25 bar partial pressure of hydrogen and comparative fast-pyrolysis experiments at 25 bar partial pressure of helium. At these process conditions, there were no significant differences in the product distribution between fast-hydropyrolysis and fast-pyrolysis of cellulose. The APCI-MS spectra for the liquid products for both the runs showed little to no differences in the types of molecules produced. These experiments formed the baseline for comparison with experiments in the presence of candidate HDO catalysts in high-pressure, fast-hydropyrolysis experiments (Tasks B.2), as explained in the next section.

[B.2] Model Compounds Study - Catalytic testing and development - I for fast-pyrolysis

High-Pressure, Continuous-Flow Fast-hydropyrolysis Reactor

In quarter FY12-Q1, experiments for high-pressure fast-hydropyrolysis of cellulose with candidate HDO catalysts for Tasks B.2 were started. From our standalone secondary fixed-bed reactor system studies (Task B.3 completed in FY11-Q4) Pt and Ru-based supported metal catalysts seemed promising. In FY12-Q1, a 2% Pt/Al_2O_3 HDO catalyst was tested and compared with previously reported results of cellulose fast-hydropyrolysis without a HDO catalyst (performed as part of Task B.1). In FY12-Q2, we tested a 2% Ru/Al_2O_3 as HDO catalyst after cellulose fast-hydropyrolysis. Both catalysts promoted C-C bond hydrogenolysis reactions such as decarbonylation and methanation that led to loss of carbon to the gas phase as CO or CH_4 respectively. In FY13-Q2, Al_2O_3 was tested as a candidate HDO catalyst, which revealed that acidity without the metal function led to significant coking with no improvement in deoxygenation. The B.ML.2 milestone (Minimum 35% weight reduction of oxygen in the liquid product as compared to the feed) was not met with any of these catalysts.

Further testing of the 2% Pt/Al_2O_3 and Al_2O_3 catalysts was done in an attempt to increase the extent of hydrodeoxygenation in the liquid product along with improving the carbon recovery in the liquid phase. In FY12-Q4 and FY13-Q2, results were reported from experiments with a 2% Pt/Al_2O_3 catalyst and Al_2O_3 catalyst, respectively, which were performed at lower catalyst weight hourly space velocity (WHSV, weight of feed per hour per unit weight of catalyst) of ~2.3 hr^{-1}. These experimental results showed further progress towards the B.ML.2 milestone, but still did not meet the 35% target weight reduction in oxygen in the liquid product as compared to the feed. The results from the low WHSV (~2.3 hr^{-1}) experiments were compared with the high WHSV (~9 hr^{1}) experimental results reported in FY 12-Q1.

In the search for better catalysts for improving the extent of deoxygenation and selectivity for C-O bond hydrogenolysis, we chose a 5 wt% PtMo (atomic ratio 1:1) supported on multi-walled carbon nanotubes (MWCNT) as a candidate HDO catalyst. Pt was chosen for its hydrogenation function and Mo was chosen as an oxophillic promoter. The results show that this PtMo catalyst led to complete deoxygenation of the cellulose fast-hydropyrolysis vapors to produce C_1-C_{8+} hydrocarbons, which met the B.ML.2 milestone. The B.ML.2 milestone has also been met with the micro-batch fast-hydropyrolysis reactor, as reported in FY-13 Q2, by complete deoxygenation of cellulose fast-hydropyrolysis vapors using the candidate HDO catalysts 2%Pt/ZrO_2 and 2%Ru/ZrO_2.

Experimental Methods

All the experiments were carried out on the high-pressure, cyclone-type, fast-hydropyrolysis reactor system (Figure 1). The feedstock for these experiments was

microcrystalline cellulose with mean particle size 50 μm (Sigmacell cellulose, Type 50). After pyrolysis, the vapor products passed through the on-stream catalytic fixed-bed HDO reactor with candidate HDO catalysts like 2% Pt/Al_2O_3 (2.5 mm diamter trilobes from Alfa Aesar), 2% Ru/Al_2O_3 (3.2 mm diameter trilobes from Alfa Aesar), γ-Al_2O_3 (1.8mm diameter extrudates from Sasol) and in-house-prepared 5wt% PtMo(1:1)/MWCNT catalyst. The 2% Pt/Al_2O_3 and 2% Ru/Al_2O_3 catalysts were reduced, *in situ at* 375 °C, and 5 wt% PtMo(1:1)/MWCNT was reduced, *in situ at* 450 °C, in a hydrogen atmosphere before the experiment. The upgraded pyrolysis vapors then moved through a concentric tube condenser, which cooled the vapors to below room temperature, and a trap cooled by a mixture of ice and water. Condensed vapors were separated from permanent gases by a coalescing filter and the liquid products were collected in the traps. A sample of the exhaust gases was analyzed with a gas chromatograph (GC) with a thermal conductivity detector (TCD) to measure the composition of CO, CO_2, H_2, CH_4 and C_2H_4 in the permanent gas products (using nitrogen internal standard) and a Flame Ionization Detector (FID) was used to analyze the C_2-C_{8+} hydrocarbons from the experiment with 5 wt% Pt Mo(1:1)/MWCNT. The collected liquid products (organics + water) were analyzed by elemental analysis to determine C/H/O content and Karl Fischer titration to determine the water content. Both analyses were used to evaluate the liquid product oxygen content (on a dry basis) and the percentage weight reduction in the oxygen content in the liquid product as compared to the feed cellulose.

In quarter FY12-Q1, experiments for high-pressure fast-hydropyrolysis of cellulose with candidate HDO catalysts for Tasks B.2 were started. From our standalone fixed-bed reactor system studies (Task B.3 completed in FY11-Q4) Pt and Ru-based supported metal catalysts seemed promising. The summary of experimental conditions from the initial experiments with 2% Ru/Al_2O_3, 2% Pt/Al_2O_3 and base case fast-hydropyrolysis experiments without HDO catalyst are shown in Table 5. The product yields from these experiments are shown in Table 6.

The liquid yields from the fast-hydropyrolysis experiments with the Ru-based and the Pt-based HDO catalyst were lower than without the HDO catalyst. The permanent gas yields were higher in the presence of both catalysts than the base case experiment without a HDO catalyst. The methane yield was significantly higher in the presence of the Ru-based catalyst, whereas the yield of carbon monoxide was significantly higher in presence of the Pt catalyst. These results suggest that, at the tested experimental conditions, Ru favored methanation and Pt favored decarbonylation as catalytic reaction pathways. Hence, with both the catalysts there was significant loss of carbon to the gas phase. This reiterated the need for optimizing the catalyst and reaction conditions to improve carbon recovery in the liquid phase, while achieving a high degree of hydrodeoxygenation.

Table 5. Experimental conditions for cellulose fast-hydropyrolysis experiments with Ru-based, Pt-based HDO catalysts at high WHSV (~9 hr^{-1}) and without HDO catalyst.

	Fast-hydropyrolysis with 2% Ru/Al_2O_3 HDO catalyst (High WHSV)	*Fast-hydropyrolysis with 2% Pt/Al_2O_3 HDO catalyst (High WHSV)*	*Fast-hydropyrolysis without HDO catalyst (for comparison)*
Feedstock	50 µm cellulose	50 µm cellulose	50 µm cellulose
Feed rate / g min^{-1}	0.8	0.8	0.9
Total mass fed / g	48	50	41
Hydrogen flow rate / (std) L min^{-1}	9.5	9.5	34.7
Helium flow rate / (std) L min^{-1}	15.7	15.7	0
Nitrogen flow rate / (std) L min^{-1}	3.0	3.0	3.0
Total pressure / bar	27	27	27
Hydrogen partial pressure / bar	9	9	25
Helium partial pressure / bar	15	15	0
Nitrogen partial pressure / bar	3	3	2
Average pyrolysis temperature / °C	~550	~550	~480
Vapor residence time in reactor / s	2.9	2.9	2.4
HDO catalyst	2% Ru/Al_2O_3	2% Pt/Al_2O_3	-
Weight hourly space velocity / hr^{-1}	~9	~9	-
Average catalyst bed temperature / °C	~375	~375	-

Table 6. Overall mass balance for fast-hydropyrolysis experiments with and without HDO catalyst (for comparison) for cellulose as model feedstock.

	Fast-hydropyrolysis with 2% Ru/Al_2O_3 HDO catalyst (High WHSV)	*Fast-hydropyrolysis with 2% Pt/Al_2O_3 HDO catalyst (High WHSV)*	*Fast-hydropyrolysis without HDO catalyst (for comparison)*
Liquid yield / wt %	56.3	42.1	66.9
Char yield / wt %	7.0	6.9	8.3
Gas yield / wt %	23.7	31.3	5.5
CO / wt %	9.7	24.6	2.1
CO_2 / wt %	3.0	3.6	3.2
CH_4 / wt %	9.0	1.6	0.2
C_2H_4 / wt %	2.0	1.3	0
Overall Mass Balance / %	87.0	80.3	80.7

The elemental analyses and the water content of the liquid products from the experiments are shown in Table 7. The liquid product from the fast-hydropyrolysis experiment in the presence of the HDO catalysts shows higher water content and lower oxygen content, on a dry basis, as compared to the fast-hydropyrolysis experiment

without the catalyst. In the presence of the Ru-based catalyst there was a 12% weight reduction in the oxygen content of the liquid product with respect to feed cellulose, whereas there was a 16% weight reduction with the Pt-based catalyst. But, with both catalysts the milestone (B.ML.2) of 35% weight reduction in the liquid product was not met.

Table 7. Elemental analysis of liquid products produced from fast-hydropyrolysis experiments with and without HDO catalyst (for comparison) for cellulose (Empirical formula $CH_{1.667}O_{0.833}$) as model feedstock.

	Fast-hydropyrolysis with 2% Ru/Al_2O_3 HDO catalyst (High WHSV)	*Fast-hydropyrolysis with 2% Pt/Al_2O_3 HDO catalyst (High WHSV)*	*Fast-hydropyrolysis without HDO catalyst (for comparison)*
Carbon (wet basis) / wt %	27.4	26.6	39.8
Hydrogen (wet basis) / wt %	8.4	9.3	7.5
Oxygen (wet basis) by difference / wt %	64.2	64.1	52.7
Water content / wt %	45.7	47.7	18.5
Carbon (dry basis) / wt %	50.5	50.9	48.8
Hydrogen (dry basis) / wt %	6.0	7.6	6.6
Oxygen (dry basis) by difference / wt %	43.5	41.6	44.6
Empirical formula (dry basis)	$CH_{1.410}O_{0.647}$	$CH_{1.769}O_{0.614}$	$CH_{1.616}O_{0.685}$
% weight reduction in oxygen (dry basis)	11.8	15.7	9.7

In an attempt to increase the extent of hydrodeoxygenation in the liquid product along with improving the carbon recovery in the liquid phase, further testing of a 2% Pt/Al_2O_3 and a Al_2O_3 catalysts were done at lower WHSV (weight hourly space velocity) of ~2.3 hr^{-1}. The bare Al_2O_3 support was used, as an acid catalyst, to test the effect of the absence of the metal functions. A summary of the reaction conditions used in the low and high WHSV experiments are shown in Table 8. A summary of the reaction conditions used in the low (~2.3 hr^{-1}) WHSV experiments is shown in Table 8 along with the comparative high WHSV (~9 hr^{-1}) experiments. The product yields from these experiments are shown in Table 9. The elemental analyses and the water content of the liquid products from these experiments are shown in Table 10.

Table 8. Experimental conditions summary for low (~2.3 hr^{-1}) and high WHSV (~9 hr^{-1}) experiments with 2% Pt/Al_2O_3 and Al_2O_3 as HDO catalyst for cellulose fast-hydropyrolysis vapors.

	Fast-hydropyrol	*Fast-hydropyr*	*Fast-hydropyr*	*Fast-hydropyr*

	ysis with 2% Pt/Al_2O_3 HDO catalyst (Low WHSV)	*olysis with 2% Pt/Al_2O_3 HDO catalyst (High WHSV)*	*olysis with Al_2O_3 as HDO catalyst (Low WHSV)*	*olysis with Al_2O_3 as HDO catalyst (High WHSV)*
Feedstock	50 µm cellulose	50 µm cellulose	50 µm cellulose	50 µm cellulose
Feed rate / g min^{-1}	0.4	0.8	0.4	0.7
Total mass fed / g	48.4	50	46.4	45.4
Hydrogen flow rate / (std) L min^{-1}	9.5	9.5	9.5	9.5
Helium flow rate / (std) L min^{-1}	15.7	15.7	16.0	15.7
Nitrogen flow rate / (std) L min^{-1}	3.0	3.0	3.0	3.0
Total pressure / bar	27	27	27	27
Hydrogen partial pressure / bar	9	9	9	9
Helium partial pressure / bar	15	15	15	15
Nitrogen partial pressure / bar	3	3	3	3
Average pyrolysis temperature / °C	~480	~550	~480	~550
Vapor residence time in reactor / s	3.2	2.9	3.1	2.9
HDO catalyst	2% Pt/Al_2O_3	2% Pt/Al_2O_3	Al_2O_3	Al_2O_3
Weight hourly space velocity / hr^{-1}	~2.3	~9	~2.3	~9
Average catalyst bed temperature / °C	~375	~375	~365	~375

With the 2% Pt/Al_2O_3 catalyst, the liquid yield from the low WHSV experiment was lower than the high WHSV experiment. The low WHSV led to higher decarbonylation, i.e. loss of carbon to gas phase as carbon monoxide, and lower liquid recoveries. The low WHSV, as compared to the high WHSV, resulted in a marginal improvement from 16% to 18% weight reduction in the oxygen content of the liquid product as compared to feed cellulose, but did not meet the milestone B.ML.2 for 35% weight reduction in oxygen content of the liquid product. The improvement in the extent of hydrodeoxygenation in the liquid product of the low WHSV relative to the high WHSV run was only marginal due to the loss of carbon to the gas phase via the Pt catalyzed decarbonylation pathway, instead of retaining the deoxygenated carbon in the liquid phase via hydrogenolysis of C-O bonds.

With Al_2O_3, at low and high WHSV, there was significant coking on the catalyst surface. The main difference in the product yields was that the coke yield on the catalyst was

higher at low WHSV and hence the liquid yield was lower as compared to the high WHSV experiments. The liquid product from the low WHSV experiment had higher water content as compared to the high WHSV experiment, showing that there was more dehydration at low WHSV as compared to high WHSV. But both experiments showed similar ~10% weight reduction in oxygen content in the liquid product as compared to feed, which does not meet the milestone (B.ML.2). The main observation from these experiments was that Al_2O_3, an acid catalyst, cokes in the absence of a metal hydrogenation function. The acid catalyst leads to dehydration of alcohols to form olefins that tend to polymerize to form coke without a metal function to hydrogenate the olefin. But, the reactions such as decarbonylation and methanation that led to loss of carbon to gas phase, due to the C-C hydrogenolysis activity of the metal function, were absent in these experiments. These experiments reveal the importance of an optimum balance of metal and acid functions needed in the HDO catalysts to improve extents of deoxygenation with high carbon recoveries in the liquid and to avoid coking of the catalyst.

Table 9. Overall mass balance for low (~2.3 hr^{-1}) and high WHSV (~9 hr^{-1}) experiments with 2% Pt/Al_2O_3 and Al_2O_3 as HDO catalyst for cellulose as model feedstock.

	Fast-hydropyrolysis with 2% Pt/Al_2O_3 HDO catalyst (Low WHSV)	*Fast-hydropyrolysis with 2% Pt/Al_2O_3 HDO catalyst (High WHSV)*	*Fast-hydropyrolysis with Al_2O_3 as HDO catalyst (Low WHSV)*	*Fast-hydropyrolysis with Al_2O_3 as HDO catalyst (High WHSV)*
Liquid yield / wt %	32.5	42.1	57.9	63.6
Char yield / wt %	4.8	6.9	19.2	13.1
Gas yield / wt %	43.1	31.3	12.7	13.3
CO / wt %	29.5	24.6	5.7	7.5
CO_2 / wt %	7.0	3.6	6.7	5.2
CH_4 / wt %	4.6	1.6	0.4	0.5
C_2H_4 / wt %	2.0	1.3	0.1	0.2
Overall Mass Balance / %	80.3	80.3	89.9	90.0

Table 10. Elemental analysis of liquid products produced from low (~2.3 hr^{-1}) and high WHSV (~9 hr^{-1}) experiments with 2% Pt/Al_2O_3 and Al_2O_3 for cellulose (Empirical formula $CH_{1.667}O_{0.833}$) as model feedstock.

	Fast-hydropyrolysis with 2% Pt/Al_2O_3 HDO catalyst (Low WHSV)	*Fast-hydropyrolysis with 2% Pt/Al_2O_3 HDO catalyst (High WHSV)*	*Fast-hydropyrolysis with Al_2O_3 as HDO catalyst (Low WHSV)*	*Fast-hydropyrolysis with Al_2O_3 as HDO catalyst (High WHSV)*
Carbon (wet basis) / wt %	10.5	26.6	28.2	34.3
Hydrogen (wet basis) / wt %	10.5	9.3	7.8	7.6
Oxygen (wet basis) by difference / wt %	79.0	64.1	63.9	58.0
Water content / wt %	79.7	47.7	43.4	31.1
Carbon (dry basis) / wt %	51.8	50.9	49.9	49.8
Hydrogen (dry basis) / wt %	7.9	7.6	5.3	6.0
Oxygen (dry basis) by difference / wt %	40.3	41.6	44.8	44.2
Empirical formula (dry basis)	$CH_{1.813}O_{0.584}$	$CH_{1.769}O_{0.614}$	$CH_{1.26}O_{0.68}$	$CH_{1.45}O_{0.67}$
% weight reduction in oxygen (dry basis)	18.3	15.7	9.1	10.5

In the search for better catalysts for improving the extent of deoxygenation and selectivity for C-O bond hydrogenolysis, we chose 5 wt% PtMo (atomic ratio 1:1) supported on multi-walled carbon nanotubes (MWCNT) as a candidate HDO catalyst. The experimental conditions and overall product distribution for cellulose fast-hydropyrolysis with 5wt% PtMo (1:1)/MWCNT as the HDO catalyst are shown in Tables 11 and 12, respectively. The results show that this PtMo catalyst led to complete deoxygenation of the cellulose fast-hydropyrolysis vapors to produce C_1-C_{8+} hydrocarbons, which meets the B.ML.2 milestone. The product distribution indicates that this catalyst has improved selectivity towards C-O hydrogenolysis products. The C_{4+}

yield is ~36 wt% of the carbon as compared to feed cellulose. Levoglucosan, which is the major product from cellulose fast-hydropyrolysis, has a six-carbon backbone and hence, its conversion to hydrocarbons in the liquid product range (C_{4+}) requires minimization of C-C hydrogenolysis.

In summary, the B.ML.2 milestone (Minimum 35% weight reduction of oxygen in the liquid product as compared to the feed) was met in the cyclone-type lab-scale fast-hydropyrolysis reactor system using a 5 wt% PtMo (1:1) /MWCNT catalyst. The B.ML.2 milestone was also met with the micro-batch fast-hydropyrolysis reactor, as reported in FY-13 Q2, with the candidate HDO catalysts 2%Pt/ZrO_2 and 2%Ru/ZrO_2.

Table 11. Experimental conditions summary for cellulose fast-hydropyrolysis with on-stream 5wt% Pt Mo/MWCNT as HDO catalyst.

Feedstock	50 µm cellulose
Feed rate / g min^{-1}	0.3
Total mass fed / g	17
Hydrogen flow rate / (std) L min^{-1}	19.5
Nitrogen flow rate / (std) L min^{-1}	1.5
Total pressure / bar	27
Hydrogen partial pressure / bar	25
Nitrogen partial pressure / bar	2
Average pyrolysis temperature / °C	~480
Vapor residence time in reactor / s	~4
HDO catalyst	5 wt% PtMo (1:1) /MWCNT
Weight hourly space velocity / hr^{-1}	~11.5
Average catalyst bed temperature / °C	~350

Table 12. Overall product distribution for cellulose fast-hydropyrolysis with 5wt% PtMo (1:1)/MWCNT as HDO catalyst.

CO / % wt of carbon in feed	19.1
CO_2 / % wt of carbon in feed	2.2
Char / % wt of carbon in feed	18.9
Product Hydrocarbons / % wt of carbon in feed	
C_1	4.4
C_2	4.5
C_3	5.1
C_4	7.3
C_5	12.5
C_6	14.4
C_7	0.6
C_{8+}	0.9
Overall Carbon Balance	89.9

Micro-batch, Fast-hydropyrolysis Reactor

The micro scale batch reactor was developed with unique capabilities such as direct analysis from a high-pressure batch reactor into a GC/MS. These capabilities were employed for analysis of pyrolysis product distributions and catalysts screening. Lab-scale reactors have a longer turn-around time, and hence a micro-scale reactor was vital in identifying candidate catalysts for further testing in the large scale reactors. This reactor offered flexibility of testing a variety of feedstocks with relative ease on a single catalyst. Model compounds, mixture of model compounds, cellulose and biomass were tested in the micro scale batch reactor as part of Tasks B.2, B.3, B.4 and C.2. A successful upgrading strategy for producing fuel range molecules from cellulose and biomass was demonstrated using the 2%Pt/ZrO_2 catalyst.

Catalytic upgrading of cellulose pyrolysis vapors in the micro-scale batch reactor was studied as part of Task B.2 in FY13-Q1to meet oxygen reduction milestone B.ML.2 (Minimum 35% weight reduction of oxygen in liquid product made from a model biomass compound using high-pressure fast-hydropyrolysis with or without a HDO catalyst as compared to conventional pyrolysis in inert atmosphere). Cellulose hydropyrolysis vapors consist of hundreds of chemical compounds, and upgrading them to desired products is a significant challenge. Model compounds have previously been used to identify useful intermediates/products and to study reaction pathways. However, a similar study on the complex mixture of pyrolysis products to determine intermediates and reaction pathways would be complicated by the number of compounds present. Therefore, the upgrading of hydropyrolysis products was carried out at complete conversion by loading excess of catalyst to simplify the product distribution to final products only. Typical catalyst-to-feed ratios used for the results reported are in the range 18 to 22. These experiments were aimed at screening catalysts to determine which catalyst gave the most desirable product distribution (C_4+) at 100% conversion. This information, along with catalyst results from the standalone secondary HDO reactor as part of Task B.3, were used for identifying future candidate catalysts for further study in the lab scale high-pressure fast-hydropyrolysis reactor for Tasks B.2 and C.2.

2% Ru/ZrO_2 and 2% Pt/ZrO_2 catalysts were studied for hydrodeoxygenation of dihydroeugenol in the standalone secondary HDO reactor and were found to be selective for removal of oxygen at 25 bar H_2 pressure (Task B.3 completed in FY11-Q4). Based on the success of these catalysts for the lignin-based model compound dihydroeugenol, experiments were carried out in FY13-Q2 for upgrading of cellulose hydropyrolysis vapors over 2% Ru/ZrO_2 and 2% Pt/ZrO_2 catalysts at 25 bar H_2 partial pressure and 300°C catalyst bed temperature. A 23 mg charge of the catalyst was loaded in the fixed-bed reactor downstream of the pyrolysis region in the pyroprobe. A known mass of cellulose was pyrolyzed at a temperature of 500°C in the pyroprobe and pyrolysis vapors were passed over the catalyst in the fixed-bed HDO reactor. The catalytically upgraded products were identified in the GC/MS, and quantified by comparing the FID signal to the standard calibration for the corresponding compounds. Standard calibration was obtained by injecting known quantities of compounds in the GC/MS and plotting the FID peak area as a function of the amount of compound injected.

The products observed after upgrading have been listed in Table 13. These products have been grouped depending on the number of carbon atoms per molecule, and the product distribution for both catalysts has been shown in Table 14.

Table 13. Products observed during upgrading of cellulose hydropyrolysis vapors over 2% Pt/ZrO_2 and 2% Ru/ZrO_2 catalysts.

Groups	Products
C_1	CO,methane
C_2	ethane
C_3	propane
C_4	butane, Isobutane
C_5	Cyclopentane, 2-Methylbutane, n-Pentane
C_6	Methylcyclopentane, Cyclohexane, 2-Methylpentane, Hexane
C_7	Methylcyclohexane, Ethylcyclopentane, 3-Methylhexane, Heptane

Table 14. Product distribution represented as carbon percentage with respect to the total carbon in the cellulose. Product distribution upgrading of cellulose hydropyrolysis vapors in the micro-batch fast-hydropyrolysis reactor over a 2% Pt/ZrO_2 catalyst (23mg) and 2% Ru/ZrO_2 catalyst (23mg) at H_2 partial pressure of 25 bar and temperature of catalyst bed at 300°C.

Catalyst	2% Ru/ZrO_2	2% Pt/ZrO_2
CO	0.0	10.2
CH_4	31.3	6.0
C_2	18.9	10.2
C_3	13.5	8.6
C_4	7.4	9.1
C_5	5.0	11.3
C_6	3.5	10.7
C_7	2.2	3.9
others	1.6	3.8
Char*	14.4	17.0
Total	97.9	91.0

* assumption – 80% of the char is composed of carbon.

The product distribution indicates a higher molecular weight distribution over the 2% Pt/ZrO_2 catalyst as compared to the 2% Ru/ZrO_2 catalyst. Methane was the major product over 2% Ru/ZrO_2 catalyst, which indicated a significant degree of C-C bond hydrogenolysis. The cellulose monomer has a six-carbon backbone and conversion to compounds in the liquid product range (C_4+) would require minimizing the C-C bond

cleavage. The 2% Pt/ZrO_2 catalyst is better than the 2% Ru/ZrO_2 catalyst, however significant improvement is needed to increase the selectivity to the desired products of C_4+ compounds.

The cellulose fast-hydropyrolysis experiments in the micro-batch fast-hydropyrolysis reactor, with candidate HDO catalysts 2%Pt/ZrO_2 and 2%Ru/ZrO_2, have shown that it is possible to achieve 100% deoxygenation of cellulose fast-hydropyrolysis vapors, using high catalyst-to-feed ratios of ~20. These experiments met the B.ML.2 milestone (minimum 35% weight reduction of oxygen in liquid product made from a model biomass compound using high-pressure fast-hydropyrolysis with or without a HDO catalyst as compared to conventional pyrolysis in inert atmosphere). These experiments have shown that it would be possible to achieve greater extents of deoxygenation in the lab-scale continuous reactor by moving to lower WHSV (or higher catalyst-to-feed rate ratios). This was demonstrated with greater degree of deoxygenation over the 5% PtMo (1:1)/MWCNT-r catalyst in the lab scale continuous reactor as a part of the report during FY13-Q3. These results have demonstrated significant progress in the catalyst development for hydrodeoxygenation of cellulose and biomass pyrolysis products and the ability to generate fuel grade molecules from these feedstocks. We have been successful in not only meeting the milestone (35% weight reduction in oxygen in liquid) but significantly improving the selectivity to C4+ fuel range molecules with the 5% PtMo (1:1)/MWCNT-r catalyst.

[B.3] Model Compounds Study - Catalyst testing and development - II for 2nd stage HDO

Standalone Secondary HDO Reactor for Model Compound Studies

In quarter FY10-3, hydrodeoxygenation (HDO) studies in the standalone fixed-bed reactor were performed at atmospheric pressure using a variety of catalysts on the lignin-derived model compound eugenol (2-methoxy-4-(2-propenyl)phenol). The goal of these studies was to understand how various catalysts performed at removing specific oxygen functional groups on individual compounds found in pyrolysis oil. The results of these atmospheric pressure studies showed that for all catalysts tested (two HZSM-5 catalysts with Si to Al ratios of 30 and 80, 1 wt% Pt on Al_2O_3, 2 wt% Ru on ZrO_2, and a sulfided 3 wt% Co and 12 wt% Mo on Al_2O_3), the desired level of HDO activity was not achieved (Task B.LM.1 milestone metric of 35 wt% reduction of oxygen in a model bio-oil compound with at least 20% oxygen). Multiple studies in the literature suggest that HDO activity is higher at elevated pressures; therefore during quarter FY10-4 the standalone fixed-bed reactor system was modified to allow for use of high-pressure hydrogen.

In quarter FY11-1, eugenol hydrodeoxygenation studies were preformed in high-pressure hydrogen using two of the same catalysts (2 wt% Ru on ZrO_2 and sulfided 3 wt% Co and 12 wt% Mo on Al_2O_3) tested at atmospheric pressure to evaluate the effect of high-pressure hydrogen. The 2 wt% Ru on ZrO_2 catalyst showed desirable HDO activity. With this catalyst, conversion of eugenol, which contains 20 wt% oxygen,

to 4-propyl-phenol as the main product resulted in a 40 wt% reduction in oxygen. This oxygen weight reduction met milestone B.LM.1 (35 wt% reduction of oxygen in a model bio-oil compound with at least 20% oxygen). Due to the promising nature of this Ru catalyst result, in quarter FY11-2 further reactions using eugenol were conducted on Ru containing catalysts.

The desired HDO products from eugenol; 4-propyl-phenol, propylbenzene, 4-(2-propenyl)-phenol, and 2-propenylbenzene, are shown in Figure 5. The products 4-propyl-phenol and 4-(2-propenyl)-phenol occur via cleavage of the methoxy side group and result in a 40 wt% reduction in oxygen from eugenol. The most desired products are propylbenzene and 2-propenylbenzene. These products result from complete deoxygenation of the model compound eugenol. The goal of these model compound catalyst studies were to find a catalyst and conditions that optimize formation of propylbenzene and 2-propenylbenzene.

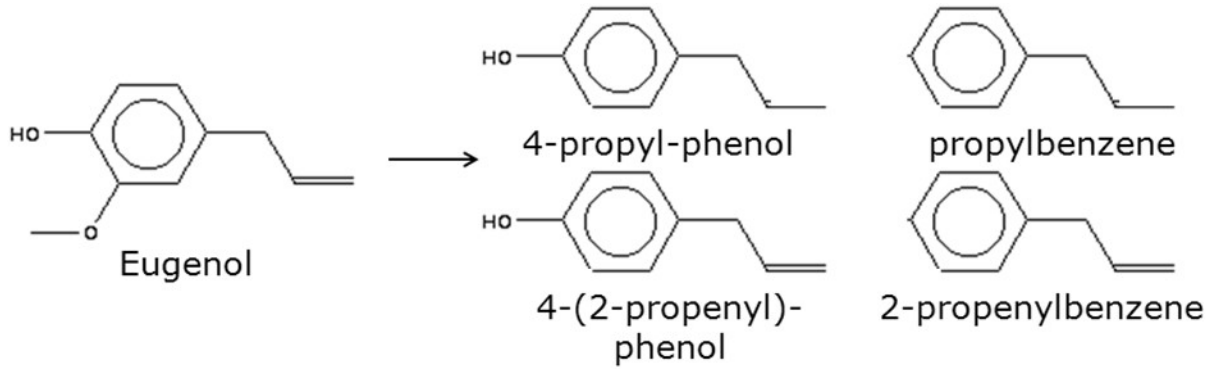

Figure 5. The desired HDO products from eugenol: 4-propyl-phenol, propylbenzene, 4-(2-propenyl)-phenol, and 2-propenylbenzene.

High-pressure hydrogen studies on eugenol were preformed with the following catalysts: 2%Ru/ZrO_2 , 1%Ru/TiO_2, 3%Ru/CeO_2, and 1.5%Ru12%Fe/Al_2O_3. All studies were conducted at 55 bar hydrogen over a temperature range of 300-450°C with ~0.3-1.4 mole percent eugenol in the vapor phase. For the 2 wt% Ru on ZrO_2 catalyst, eugenol was reacted at 55 bar hydrogen over a temperature range of 320-450°C with ~0.3 mole percent eugenol in the vapor phase. The major product was 2-methoxy-4-propyl phenol, which occurs via saturation of the double bond on the propenyl side chain. This product is not a desired HDO product. The second major product was 4-propyl-phenol, which occurs via cleavage of the oxygen-containing methoxy side group on the aromatic ring of eugenol and saturation of the propenyl side chain. The minor products produced are isoeugenol (resulting from isomerization of the propenyl side chain of eugenol), and the desirable HDO products propylbenzene and propylcyclohexane. Propylcyclohexane is a desirable product because of the complete removal of oxygen, but it also uses extra hydrogen to saturate the ring. The conversion of eugenol to the desired HDO products of 4-propyl-phenol, propylbenzene and

propylcyclohexane increased as the temperature increased, as can be seen in Figure 6, giving ~23% HDO products (as determined from GC peak areas) at 400°C.

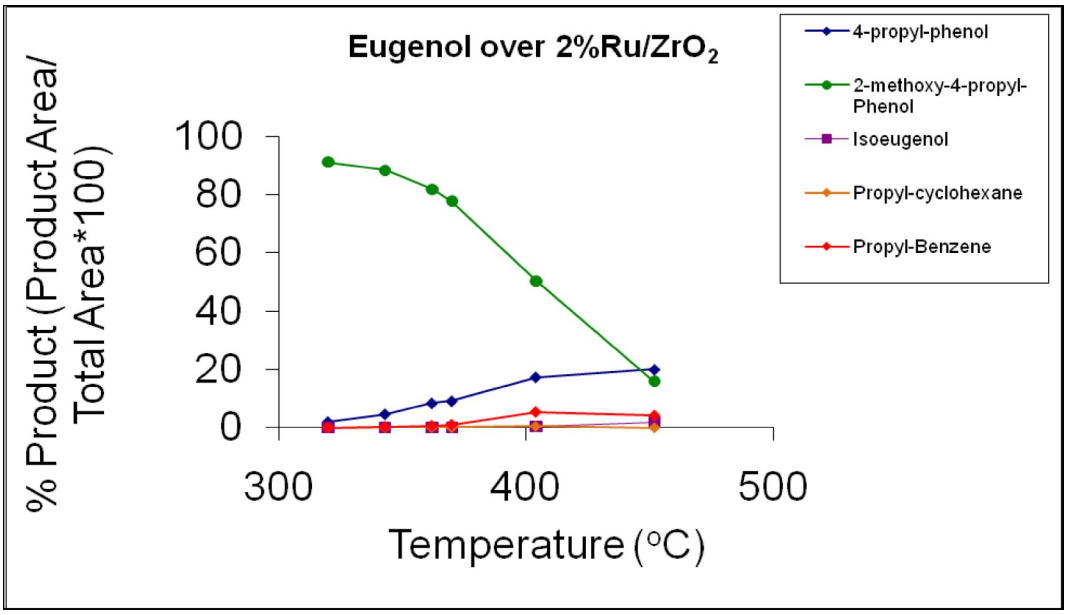

Figure 6. Product percentage produced as a function of reaction temperature for the reaction of eugenol over a 2 wt% Ru on ZrO_2 catalyst.

Hydrodeoxygenation reactions of eugenol were also studied on other Ru based catalysts, 1%Ru/TiO_2, 3%Ru/CeO_2, and 1.5%Ru12%Fe/Al_2O_3, at 55 bar hydrogen over a temperature range of 300-450°C with ~0.3-1.4 mole percent eugenol in the vapor phase. For the 1%Ru/TiO_2 catalyst, the major products at 300°C were 2-methoxy-4-propyl phenol and isoeugneol, both undesirable products. However, at 400°C and above, the major product becomes the desired HDO product 4-propyl-phenol, produced at 27% (as determined from GC peak areas) a shown in Table 15. For the 3%Ru/CeO_2 catalyst, the major product at 320°C was 2-methoxy-4-propylphenol. Three HDO products were formed: 4-propyl-phenol, propylbenzene and propylcyclohexane. This catalyst, out of those studied, had the highest formation of the fully deoxygenated products propylbenzene and propylcyclohexane at 320°C. For the 1.5%Ru12%Fe on Al_2O_3 catalyst, the temperature range 350-400°C gave the best deoxygenation result, with the major product being 4-propyl-phenol. The deoxygenated product propylbenzene was also formed above 400°C. Undesirable products 2-methoxy-4-propylphenol and isoeugenol were also formed. At 400°C, the HDO products 4-propyl-phenol and propylbenzene were produced at 35% (as determined from GC peak areas).

Recalling that the most desired HDO product from eugenol is the fully deoxygenated compound propylbenzene, the 2%Ru/ZrO_2 and 1.5%Ru12%Fe/Al_2O_3 catalysts appear promising as they gave the highest percent of propylbenzene, as can be seen in Table 15. However, reaction conditions and the percent of eugenol in the vapor phase varied for the catalysts tested, and a true comparison of the four catalysts cannot be drawn.

Additionally, the double bond on the propenyl side chain of the model compound eugenol reacts to form undesirable products (such as isoeugenol), which complicates the analysis without providing any information on HDO activity. In the future, reactions were run using a compound similar to eugenol, 2-methoxy-4-propylphenol, which is identical to the structure of eugenol except that the double bond is saturated to give a propyl side group. Therefore, reactions using dihydroeugenol will allow for a determination of the catalysts hydrodeoxygenation activity versus hydrogenation activity with minimal complicating side reactions.

Table 15. Percent of major and minor products for eugenol over four Ru catalysts in 55 bar hydrogen pressure.

Catalyst	% Eugenol in Vapor phase	Peak Area % 2-methoxy-4-propyl-phenol	Peak Area % isoeugenol	**Peak Area % 4-propyl-phenol**	**Peak Area % propyl-benzene**	**Total Deoxygenated Peak Area %**
1%Ru/TiO_2	0.7	16.92	10.55	26.65	X	**26.65**
2%Ru/ZrO_2	0.3	50.39	0.48	17.37	5.33	**22.69**
3%Ru/CeO_2 **At 325°C	1.4	54.87	X	4.28	1.68	**5.96**
1.5%Ru12%Fe/ Al_2O_3	0.7	23.13	5.91	32.78	2.536	**35.30**

All percentages are for reactions at 400°C, except for the 3 wt% Ru on CeO_2 catalysts, which is given for 320°C. The desired HDO products 4-propyl-phenol and propylbenzene are in bold, and the total percent of deoxygenated products is given.

In quarter FY11-3, in-depth kinetic studies were performed on the 2%Ru/ZrO_2 catalyst using the model compound dihydroeugenol (2-methoxy-4-propylphenol). The desired HDO products from dihydroeugenol, 4-propyl-phenol and propylbenzene, are shown in Figure 7. The product 4-propyl-phenol would occur via cleavage of the methoxy side group and would result in a 40 wt% reduction in oxygen from dihydroeugenol. The most desired product would be propylbenzene, which would result from complete deoxygenation of the model compound dihydroeugenol.

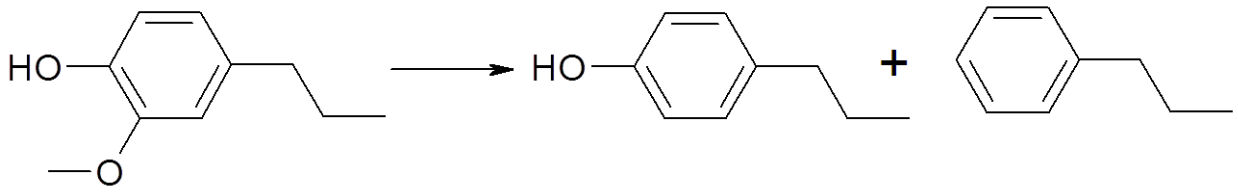

Figure 7. The desired HDO products from dihydroeugenol: 4-propyl-phenol and propylbenzene.

While the 2%Ru/ZrO2 catalyst showed promising HDO activity, other products besides the desired HDO product 4-propyl-phenol and propylbenzene were produced and the completely deoxygenated product propylbenzene was a minor product. Therefore, in FY11-4, as part of continued work on Task 2.C to identify a catalyst with optimum selectivity towards deoxygenated products to be used in further studies as part of Tasks

B.2/B.3/B.4/B.5/C.2/C.3, further catalyst studies on the model compound dihydroeugenol were performed comparing the 2 wt% Ru/ZrO_2 catalyst with a 2 wt% Pt/ZrO_2 catalyst.

The catalyst comparison of $2\%Ru/ZrO_2$ and $2\%Pt/ZrO_2$ catalysts was performed at 24 bar hydrogen over a temperature range of 300-450°C with ~3.8 mole percent dihydroeugenol in the vapor phase. Catalysts underwent a deactivation period of 10-24 hours before data was collected to ensure that the catalysts were stable. Both the $2\%Ru/ZrO_2$ and $2\%Pt/ZrO_2$ catalysts were stable after this period, as can be seen in Figure 8.

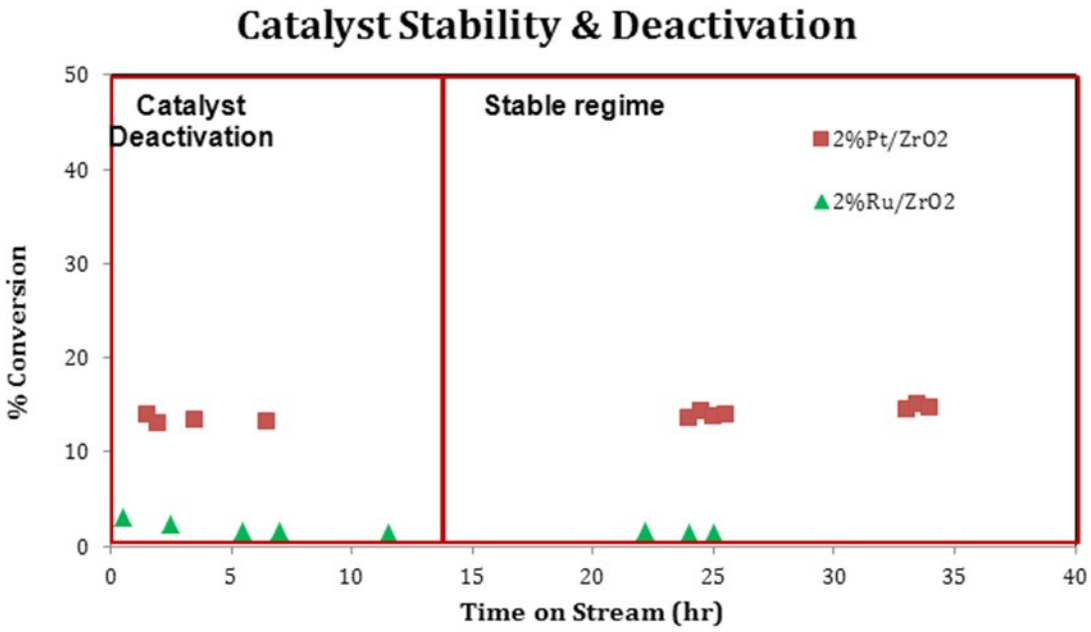

Figure 8. Catalyst stability plot showing reactant dihydroeugenol conversion versus time-on-stream. Both catalysts are stable after the deactivation period.

Table 17. Stabilized rate of reaction for the two catalysts. The rate of reaction is defined as moles of reactant consumed per mole of metal per minute. Reaction conditions are 300°C at 24 bar in 2.6 L min^{-1} H_2 and 0.06 ml min^{-1} Dihydroeugenol.

	Actual wt % (from ICP)	Initial Conversion	Stabilized Conversion	**Stabilized Rate of reaction (mol g $metal^{-1}$ min^{-1})**
$2\%Pt/ZrO_2$	0.87	14%	15%	$5.6E^{-04}$
$2\%Ru/ZrO_2$	0.58	5%	1.5%	$8.5E^{-05}$

After the catalyst activity had stabilized, the rate of reaction for the two catalysts were determined, as can be seen in Table 17. The rate of reaction is defined as moles of

reactant consumed per mol of metal per minute. The moles of metal in the catalysts were experimentally determined by ICP (Inductively coupled plasma) measurements. Reaction conditions were 300°C at 24 bar in 2.6 L min^{-1} H_2 and 0.06 ml min^{-1} Dihydroeugenol.

As Table 17 shows, the rate of reaction on the 2%Pt/ZrO_2 catalyst was **6.5** times larger than rate on the 2%Ru/ZrO_2 catalyst. While the 2%Pt/ZrO_2 catalyst has a 6.5x larger rate than the 2%Ru/ZrO_2 catalyst, this is only one measure of the catalysts overall performance. More important than the overall rate is the catalyst's selectivity towards deoxygenated products (desired products, as oxygen removal is the overall goal) versus its selectivity towards hydrogenated products (undesired products, as hydrogenation reactions consume hydrogen without removing oxygen). As a measure of the catalysts selectivity of HDO vs. hydrogenation, the selectivity ratios of the deoxygenated to hydrogenated products were compared for the two catalysts. A higher ratio is desired, as this implies greater selectivity towards the deoxygenated product without consuming hydrogen via ring hydrogenation. The two selectivity ratios, shown in Table 18, are of 1) 4-propylphenol to 4-propylcyclohexanol and 2) propylbenzene to propylcyclohexane.

Table 18. Selectivity ratios of 1) 4-propylphenol to 4-propylcyclohexanol and 2) propylbenzene to propylcyclohexane for the two catalysts, 2%Pt/ZrO_2 and 2%Ru/ZrO_2. The selectivity ratios of the two catalysts are at reaction conditions of 300°C at 24 bar in 2.6 L min^{-1} H_2 and 0.06 ml min^{-1} Dihydroeugenol.

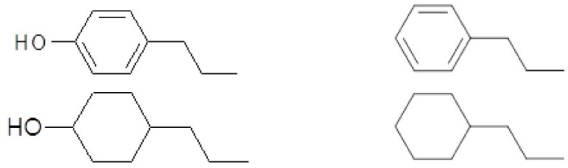

	Selectivity ratio of 4-propylphenol to 4-propylcyclohexanol	Selectivity ratio of propylbenzene to propylcyclohexane
2%Pt/ZrO_2	1.0	0.7
2%Ru/ZrO_2	57	∞

The 2%Ru/ZrO_2 catalyst has a higher selectivity ratio for both sets of deoxygenated products, showing that the ruthenium catalyst has a higher selectivity towards deoxygenation without ring hydrogenation. For the ratio of propylbenzene to propylcyclohexane on the 2%Ru/ZrO_2 catalyst, the ratio is given as infinity because no propylcyclohexane is detected.

In conclusion, both the 2%Pt/ZrO_2 and 2%Ru/ZrO_2 catalysts show deoxygenation activity, as the deoxygenated products 4-propylphenol and propylbenzene are observed. The 2%Pt/ZrO_2 showed a 6.5 times higher rate of reaction than the

2%Ru/ZrO_2 catalyst, however the 2%Ru/ZrO_2 catalyst has higher selectivity towards the desired HDO products without ring hydrogenation. Based on these promising model compound results using the lignin-derived compound dihydroeugenol, both supported Pt and Ru based catalysts will be tested in the high-pressure, fast-hydropyrolysis reactor (Task B.2, C.3, and C.3), expected to be completed by FY12.

[B.4] Model Compounds Study - Perform task B.2 and B.3 with some key model compound mixtures

Standalone Secondary HDO Reactor for Model Compound Studies

Task B.4 (catalyst testing and development of model bio-oil compound mixtures) was completed using the standalone secondary HDO reactor and the micro-batch, fast hydropyrolysis reactor in FY13Q1. It is anticipated that model compounds when fed together might exhibit interaction effects. For example, presence of one model compound may affect a reaction pathway of other model compound by occupying the relevant catalytic sites. The mixture of model compounds is chosen to represent different oxygen functional groups as well as to represent cellulose and lignin sections of biomass. This study was expected to give us a better understanding of the challenges faced when transitioning catalytic HDO from a single model compound to real conditions with biomass feed. The standalone secondary HDO reactor was used to perform kinetic studies on individual model compounds as well as model compound mixtures using furfural and acetic acid over a 5% Pt/MWCNT (multi walled carbon nanotube) catalyst. Furfural was chosen as a representative model compound from pyrolysis of cellulose and hemicellulose sections of lignocellulosic biomass. Furfural and its derivatives are known products from cellulose pyrolysis. Acetic acid was chosen to represent small oxygenates as well as a carboxylic acid functional group. A 5% Pt/MWCNT catalyst was chosen as a HDO catalyst, since Pt is known hydrogenation catalyst and MWCNT is an inert support.

The model compounds were pumped as a liquid from a HPLC pump and vaporized in-line before the catalytic reactor. A carrier gas stream (95% H_2, 5% N_2) mixed with the model compound vapor at the top of the reactor before passing over the catalyst bed. The product mixture flows to a condenser trap cooled by an ice bath where the liquid product is separated out from the gases. The permanent gas proceeds to a gas chromatograph (GC) for online analysis. The GC was an Agilent 7890A fitted with a Carboxen 1000 column for permanent gas analysis and DB-1701 column for analysis of the liquid condensate. The liquid product was removed from the condenser trap at the end of the experiment and injected in to GC for product composition analysis.

To test the impact mixtures have on the HDO of model bio-oil compounds, HDO of individual model compounds was compared with the HDO of those compounds in a mixture. Furfural HDO was tested over a 5% Pt/MWCNT catalyst. Table 19 lists the experimental conditions for the HDO of furfural.

Table 19: Experimental conditions for furfural HDO.

Parameter	Value
Furfural flow rate/ ml min^{-1}	0.2
Weight hourly space velocity/ h^{-1}	10
Temperature range/ °C	260-284
Partial pressure hydrogen/ bar	19.1
Partial pressure furfural/ bar	0.2
Partial pressure nitrogen/ bar	0.7

Table 20: Conversion and selectivity of products for the reaction of furfural in the standalone secondary HDO reactor over a 5% Pt/MWCNT catalyst at H_2 partial pressure of 19 bar and temperatures of 284-350°C.

Temperature/C	Conversion/ %	Selectivity/ %	
		Furfuryl alcohol	Furan
260	4	62	11
265	6	57	10
278	11	40	8
284	17	34	7

The major products that were observed were furfuryl alcohol and furan. These products can be hypothesized to be primary products from reduction and decarbonylation pathways respectively (Figure 9). At 260°C and under 19 bar hydrogen pressure, selectivity to furfuryl alcohol is 62% and to furan is 7%. This shows that the desirable reduction pathway is favored over the undesired decarbonylation pathway under the experimental conditions. As the temperature is increased, it is observed that selectivity to furfuryl alcohol decreases significantly (Table 20). Correspondingly, an increase in the selectivity towards ring-hydrogenated products like tetrahydrofuran and tetrahydrofurfuryl alcohol as well as 2-methyl furan is observed with increasing temperature.

Figure 9 shows a proposed reaction pathway for the HDO of furfural. Furan and furfuryl alcohol are the primary products from furfural. These primary products can further be hydrogenated to form tetrahydrofuran, 2-methyl furan and tetrahydrofurfuryl alcohol. Each of these three compounds was formed with less than 2% selectivity at 260°C. Among furan and furfuryl alcohol, the hydrogenation pathway to reduce furfural to furfuryl alcohol is selectively preferred under 19 bar H_2 pressure. This result is in contrast to the microscale pyrolysis reactor results where decarbonylation is the preferred pathway under 1 bar hydrogen pressure.

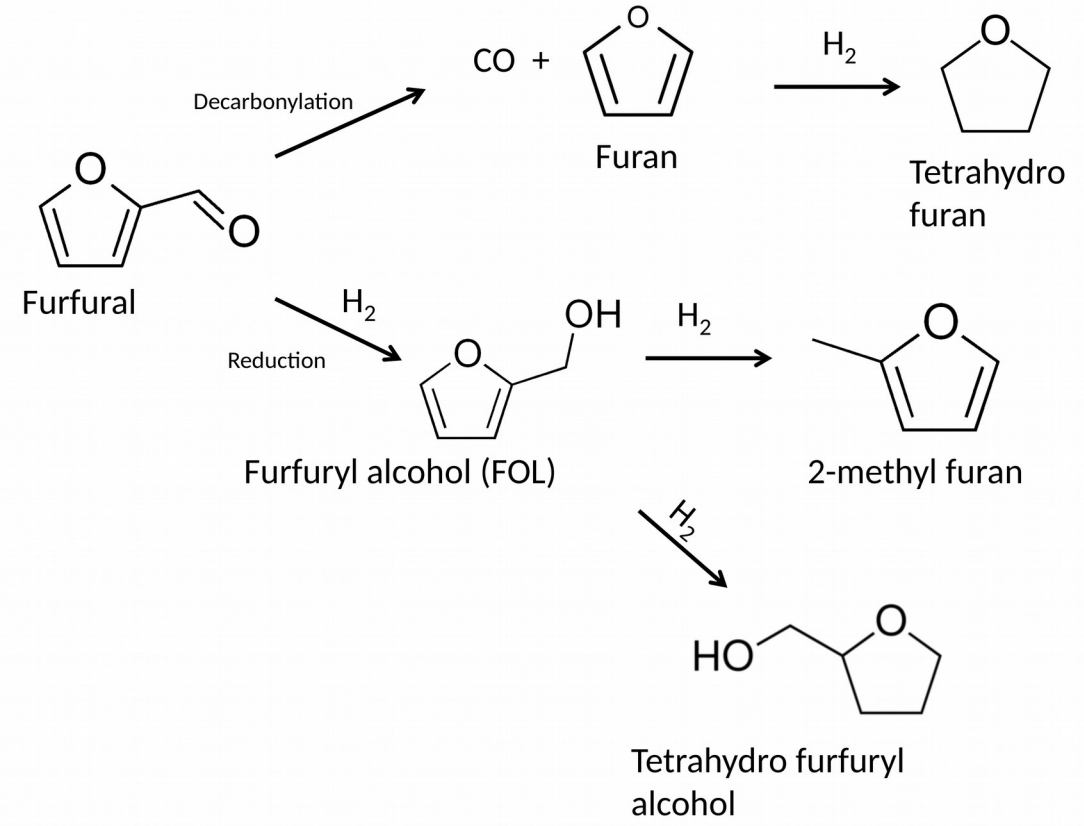

Figure 9: Possible reaction pathway for HDO of furfural.

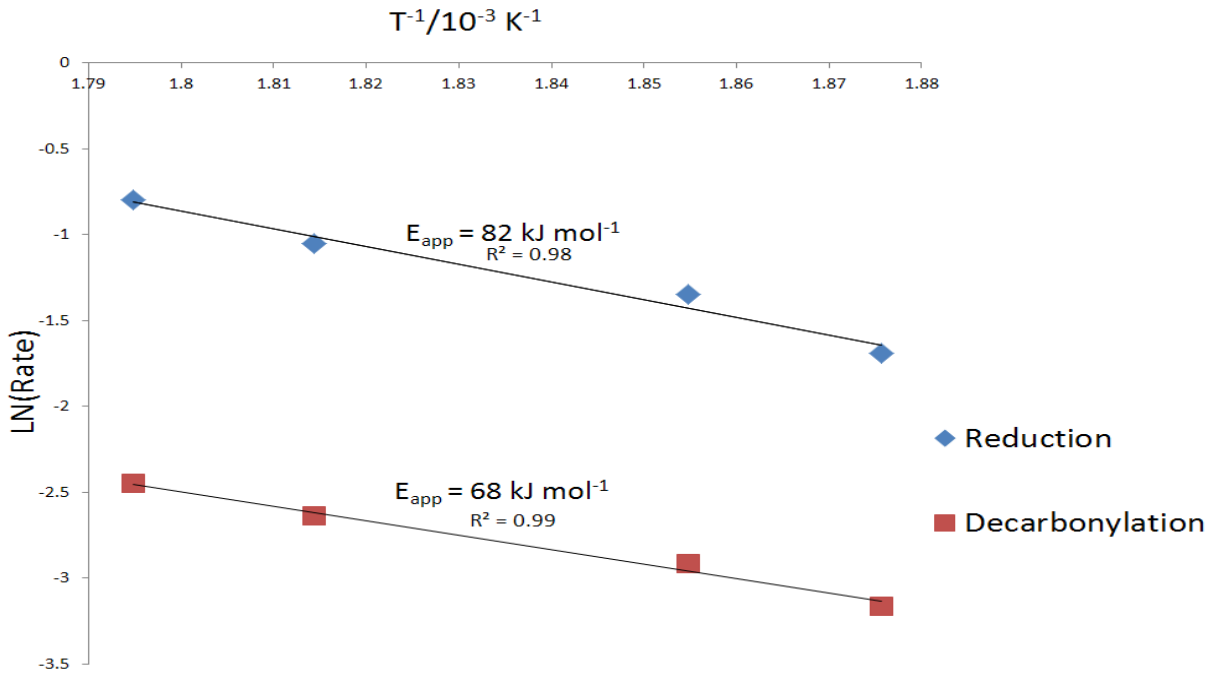

Figure 10: Arrhenius plot for reduction and decarbonylation pathways of furfural HDO.

The selectivity to various products varies with temperature, and the extent to which the selectivity varies with temperature differs for different products. This effect can be quantified by the apparent activation energy for different pathways. Apparent activation energy can be estimated from the slope in the Arrhenius plot, shown in Figure 10 below for both the decarbonylation and reduction pathways to furan and furfuryl alcohol (FOL) respectively. The decarbonylation pathway rate has been estimated using CO yield, as its measurement was done online. The rate is estimated as moles of product produced per second normalized by moles of platinum. The chosen product for reduction pathway is furfuryl alcohol and for decarbonylation pathway is carbon monoxide. The apparent activation energy to furan is about 68 kJ mol^{-1} and to FOL is 82 kJ mol^{-1}.

Additionally, HDO of the individual model compound acetic acid was tested over the 5% Pt/MWCNT catalyst. Table 21 lists the experimental conditions for the HDO reaction of acetic acid. The major products from acetic acid HDO are ethanol, carbon monoxide, methane and ethyl acetate.

Table 21: Experimental conditions for acetic acid HDO.

Parameter	Value
Acetic acid flow rate/ ml min^{-1}	0.068
Weight hourly space velocity/ h^{-1}	4
Temperature range/ °C	284-350
Partial pressure hydrogen/ bar	19.2
Partial pressure acetic acid / bar	0.1
Partial pressure nitrogen/ bar	0.7

Figure 11 shows a possible reaction pathway for acetic acid hydrodeoxygenation. Acetic acid can essentially undergo three primary reactions – decarboxylation to CO_2, dehydration to acetic anhydride, and reduction to acetaldehyde. Acetaldehyde can then decarbonylate to carbon monoxide and methane or undergo further reduction to ethanol. Ethanol can undergo esterification with acetic acid to produce ethyl acetate.

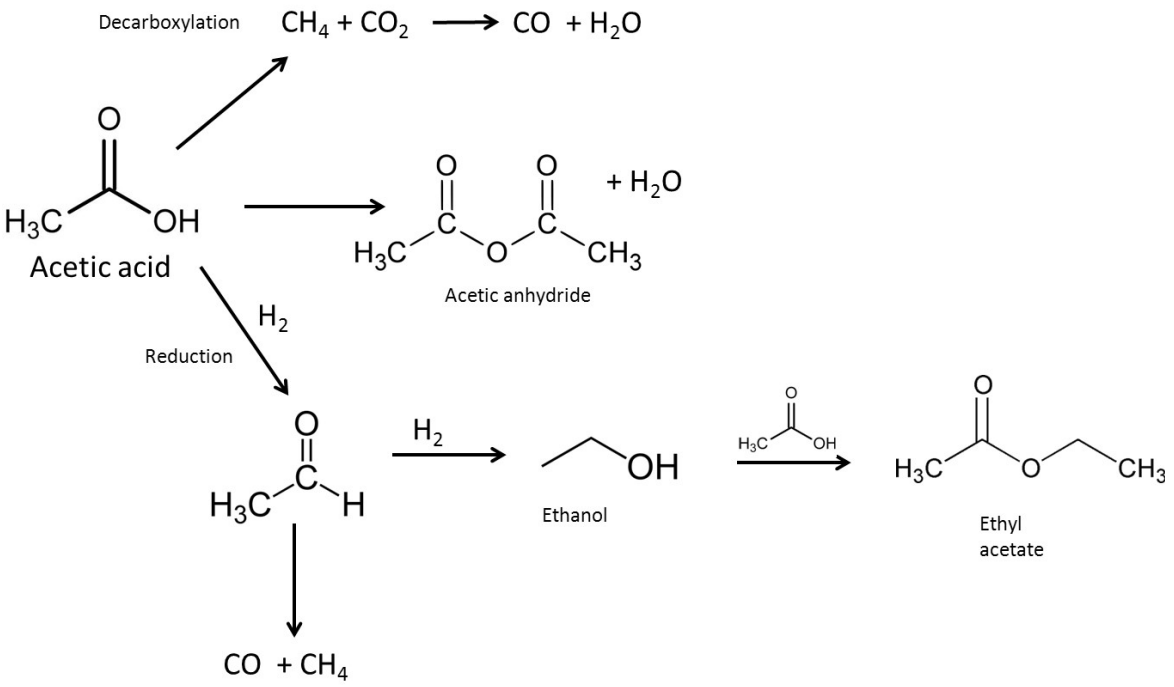

Figure 11: Possible reaction pathway for HDO of acetic acid.

Table 22 shows the conversion and selectivity of the products of acetic acid HDO for various temperatures. At 284°C, acetic acid conversion is very low and the only product observed is ethanol. As the temperature is increased, ethyl acetate is also produced. Ethyl acetate is formed by a secondary reaction between ethanol and acetic acid.

Table 22: Conversion and selectivity of products for the reaction of acetic acid in the standalone secondary HDO reactor over a 5% Pt/MWCNT catalyst at H_2 partial pressure of 19 bar and temperatures of 284-350°C.

Temperature/ °C	Total Conversion/ %	Selectivity/ %			
		Ethanol	Ethyl Acetate	Acetaldehyde	CO + CH_4
284	0.5	-	-	-	-
332	6	47	13	2	33
350	11	35	27	1	35

As seen in furfural HDO, the hydrogenation pathway is also preferred in the case of acetic acid HDO. Ethanol is the major product at all the temperatures followed by ethyl acetate. Hence, the reduction pathway to first produce acetaldehyde and then ethanol is favored. Almost no carbon dioxide was detected in the online GC analysis. This could imply that decarboxylation pathway is shut off and all the conversion happens through a

reduction to acetaldehyde with subsequent decarbonylation to carbon monoxide and methane.

To determine the impact of model bio-oil model compound mixtures, the HDO of a mixture of furfural and acetic acid was tested over the 5% Pt/MWCNT catalyst. While feeding the mixture at 284°C, the flow rate and composition of furfural-acetic acid mixture was adjusted such that the partial pressure of each reactant remained similar to the individual feed cases. At 284°C, the results show that conversion of furfural remains similar to the individual feed case, and acetic acid is recovered without any reaction. At the lower temperature range studied for these two bio-oil model compounds, no interaction effects were observed for the mixture.

Micro-batch, Fast-hydropyrolysis Reactor

Task B.4 (catalyst testing and development of model bio-oil compound mixtures) was completed using the standalone secondary HDO reactor and the micro-batch, fast hydropyrolysis reactor.

Catalyst testing for Task B.4 model compound mixture studies was carried out in the micro-batch, fast hydropyrolysis reactor using furfural, acetic acid, and dihydroeugenol as the model compounds. Furfural is representative of various compounds of fast pyrolysis having a furan ring and an aldehyde group, while acetic acid is representative of the acidic compounds in the bio-oil having a carboxylic group. Dihydroeugenol is a model compound obtained for pyrolysis of lignin fraction of biomass.

A 5% Pt/MWCNT catalyst was chosen on the basis of the standalone secondary HDO reactor studies. Experiments were carried out for the model compounds over the 5% Pt/MWCNT catalyst at 1 bar of H_2 partial pressure, and at a temperature of 210°C in the HDO reactor. 2.6 mg of the diluted catalyst (10 times dilution by MWCNT support) was loaded in the fixed-bed reactor downstream of the pyrolysis region in the pyroprobe. A known mass of model compound was vaporized at a temperature of 300°C in the pyroprobe and passed over the catalyst in the fixed-bed reactor. The catalytically upgraded products were identified in the GC/MS, and quantified by comparing the FID signal to the standard calibration for the corresponding compounds. Standard calibration was obtained by injecting known quantities of compounds in the GC/MS and plotting the FID peak area as a function of the amount of compound injected. This procedure was followed for testing the model compound mixtures as well.

The major products obtained when furfural was reacted over the 5% Pt/MWCNT catalyst at 210°C were furan, furfuryl alcohol and 2-Methyl furan (Figure 9). Identical products were observed in the standalone secondary HDO reactor for furfural HDO. 2-Methyl furan was the desired HDO product obtained by the C-O bond hydrogenolysis. Furfuryl alcohol was formed by hydrogenation of the aldehyde moiety to an alcohol group. The conversion of furfural and yield of the major products are given in Table 23. The selectivity for the hydrogenation product, furfuryl alcohol, was higher in the

standalone steady state HDO reactor due to high partial pressure of hydrogen (P_{H2}: 19.1 bar) as compared to the micro-scale batch reactor (P_{H2}: 1 bar).

Table 23. Conversion and yield of products for the reaction of furfural in the micro-batch fast-hydropyrolysis reactor/ fixed-bed HDO reactor over a 5% Pt/MWCNT catalyst (2.6mg) at H_2 partial pressure of 1 bar at 210°C.

Conversion / %	
Furfural	20.5
Yield / %	
Furan	8.8
2-Methyl furan	1.5
Furfuryl alcohol	2.2
Others	3.3
CO_2	<0.5
CO	2.5

Table 24. Conversion and yield of products for reaction of acetic acid in the micro-batch fast-hydropyrolysis reactor/ fixed-bed HDO reactor over a 5% Pt/MWCNT catalyst (2.6mg) at H_2 partial pressure of 1 bar 210°C.

Conversion / %	
Acetic acid	8.7
Yield / %	
Acetaldehyde	0.9
Ethanol	1.8
Unidentified species 1	0.4
Unidentified species 2	1.0
CO_2	2.0
CO	0.7

Table 25. Conversion and yield of products for reaction of mixture of acetic acid and furfural in the micro-batch fast-hydropyrolysis reactor/ fixed-bed HDO reactor over a 5% Pt/MWCNT catalyst (2.6mg) at H_2 partial pressure of 1 bar 210°C.

Conversion / %		**Conversion / %**	
Acetic acid	5.1	Furfural	9.2
Yield / %		**Yield / %**	
Acetaldehyde	0.5	Furan	4.6
Ethanol + Unidentified species 2	2.1	2-Methyl furan	0.4
Unidentified species 1	0.9	Furfuryl alcohol	1.0
CO_2 (total)	0.5	Others	1.5
CO (total)	2.0		

The conversion of acetic acid under similar conditions was lower than that for furfural which is a consequence of the lower rate over the catalyst, which was also observed in the standalone secondary continuous catalytic HDO reactor. The major products observed were ethanol, acetaldehyde and carbon dioxide (Table 24). Two additional minor products were also observed, but we were unable to identify them due to limitations of the MS identification database. Acetaldehyde and ethanol are hydrogenation products, while CO_2 is a product of decarboxylation reaction.

The mixture of furfural and acetic acid (0.5ul each) was passed over the catalyst. The results have been shown in Table 25. There was a decrease in conversion of both the compounds, since they were competing for sites over the catalyst. There was no significant change in selectivity/product distribution (for quantified fraction of products) from acetic acid and furfural. It was difficult to accurately estimate the selectivity for certain compounds due to difficulty in GC quantification when these products eluted at the same GC retention times, causing overlapping peaks. Also we could not differentiate between the fractions of CO produced by reaction of either compound. Acetic acid and furfural competed for sites on the catalyst resulting in a drop in conversion for both the compounds relative to individual reactions of each compound reacted over the catalyst. No other significant conclusion can be drawn from this experiment about the behavior of mixture of model compounds over a catalyst.

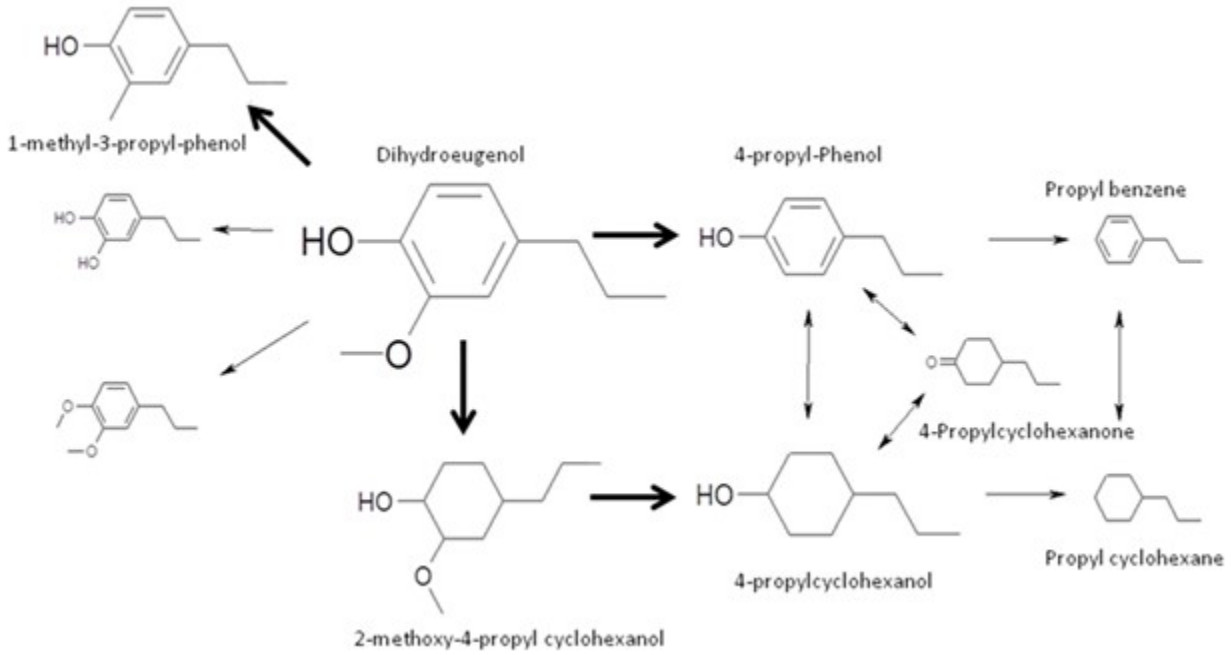

Figure 12. Proposed reaction scheme for Dihydroeugenol reacted over supported Pt catalysts.

Dihydroeugenol (DHE) was used as a model compound for pyrolysis products from the lignin fraction of the biomass. Hydrodeoxygenation (HDO) of DHE focused on removal of oxygen from the methoxy and hydroxyl group without hydrogenation of the aromatic

ring. The products have been classified under two sub groups: HDO products and ring hydrogenation products. The conversion, yield and selectivity for the products have been listed in table 26, table 27, and table 28. Selectivity of products from DHE have been compared with the results from the standalone secondary HDO reactor which have been previously reported. The experiments in the standalone steady state HDO reactor were carried out over 2% Pt/ZrO_2 catalyst at a temperature of 210°C and 23 bar partial pressure of hydrogen. Similar products were observed for both the standalone secondary HDO reactor and the micro-batch fast-hydropyrolysis reactor/ fixed-bed HDO reactor. Figure 12 shows the previously reported proposed reaction scheme for the HDO of dihydroeugenol.

Comparing the results of the standalone secondary HDO reactor and the micro-batch fast-hydropyrolysis reactor/ fixed-bed HDO reactor in Table 28, which operated at different pressures, it can be observed that higher partial pressure of hydrogen promotes the ring hydrogenation pathway. The selectivity for ring hydrogenation products is higher at P_{H2} = 23 bar as compared to P_{H2} = 1 bar. Partial pressure of hydrogen is an important factor to be considered during upgrading of pyrolysis vapors.

A mixture of furfural and dihydroeugenol (0.5ul each) was passed over the 5% Pt/MWCNT catalyst and the products were quantified. There was no significant change in the conversion of both the species; however there was a significant change in selectivity of the HDO products from DHE. As shown in table 27, selectivity for propyl benzene increased from 7.2% to 14.1% while that for 2-methoxy-4-propyl cyclohexanol decreased from 39.1% to 33%. The ring hydrogenation pathway was less favored in presence of furfural, due to competition for hydrogen adsorbed over the catalyst. The presence of furfural along with DHE changed the selectivity for the HDO pathway for DHE over 5% Pt/MWCNT catalyst.

Table 26. Conversion and selectivity of products for reaction of dihydroeugenol (DHE) in the micro-batch fast-hydropyrolysis reactor/ fixed-bed HDO reactor over a 5% Pt/MWCNT catalyst (2.6mg) at H_2 partial pressure of 1 bar 210°C.

Conversion / %	
Dihydroeugenol (DHE)	16.8
Yield / %	
Propyl cyclohexane	1.4
Propyl benzene	1.2
Unidentified	0.6
4-propylcyclohexanol	3.0
1-methyl-3-propyl-phenol	0.7
4-Propylcyclohexanone	1.1
2-methoxy-4-propyl cyclohexanol	6.6
4-propyl-Phenol	2.1

Table 27. Selectivity of products for reaction of Dihydroeugenol (DHE) and a mixture of DHE and furfural in the micro-batch fast-hydropyrolysis reactor/ fixed-bed HDO reactor over a 5% Pt/MWCNT catalyst (2.6mg) at H_2 partial pressure of 1 bar 210°C.

	Selectivity / %	
Feed	only DHE	DHE+furfural
HDO products		
Propyl benzene	**7.2**	**14.1**
1-methyl-3-propyl-phenol	**4.2**	**4.6**
4-propyl-Phenol	**12.6**	**13.9**
Ring hydrogenation products		
Propyl cyclohexane	**8.5**	**10.0**
4-propylcyclohexanol	**17.7**	**15.7**
4-Propylcyclohexanone	**6.6**	**5.1**
2-methoxy-4-propyl cyclohexanol	**39.1**	**33.0**

Table 28. Selectivity of products for reaction of Dihydroeugenol (DHE) over 5% Pt/MWCNT catalyst (2.6mg) at H2 partial pressure of 1 bar 210°C (in the micro-batch fast-hydropyrolysis reactor/ fixed-bed HDO reactor) and over 2% Pt/ZrO2 catalyst at H2 partial pressure of 23 bar 210°C (in the standalone steady state HDO reactor).

	Selectivity / %	
Partial Pressure of hydrogen/ bar	1	23
HDO products		
Benzene, propyl-	**7.2**	**0.0**
Phenol, 3-methyl-6-propyl-	**4.2**	**0.3**
Phenol, 4-propyl-	**12.6**	**1.7**
Ring hydrogenation products		
Cyclohexane, propyl-	**8.5**	**0.1**
4-propylcyclohexanol	**17.7**	**4.9**
4-Propylcyclohexanone	**6.6**	**1.5**
2-methoxy-4-propyl cyclohexanol	**39.1**	**73.6**

In summary, a mixture of model compounds representing cellulose and lignin pyrolysis were studied for HDO activity over 5%Pt/MWCNT catalyst, completing Task B.4. Partial pressure of hydrogen is an important parameter, since it influences hydrogenation pathways, especially during upgrading of lignin derived compounds. Increase in the partial pressure of hydrogen increases selectivity for desired HDO products as was observed in the case of furfural and acetic acid. It was observed that the rate for acetic acid was significantly lower over the catalyst than that for furfural under the same conditions. From the study of mixtures of model compounds it was seen that the presence of furfural decreased the selectivity for ring hydrogenation products, thereby promoting the HDO pathway for conversion of DHE.

Upgrading of biomass pyrolysis products would involve simultaneous hydrodeoxygenation of various oxygenated chemical species which would interact to modify reaction pathways over the catalyst. Similar phenomenon could be expected during upgrading of biomass pyrolysis products and poses significant challenge for catalyst development. The study of mixture of model compounds has brought to light the various parameters which need to be optimized while designing HDO catalysts and during operation of HDO reactors.

B.5] Model Compounds Study - Introduce CO along with H_2 and study B.3 and 2B.4

Standalone Secondary HDO Reactor for Model Compound Studies

Task B.5 (catalyst testing and development of model compounds while introducing CO along with H_2) was completed in quarter FY13-2 In the standalone secondary HDO reactor. The goal of this study was to understand how HDO catalysts perform in the present of H_2/CO mixtures. This is to investigate the possible integration of the H_2Bioil process with industrial processes such as methane reforming or coal power plants; where a waste stream of H_2 (with other gases such as CO) is produced that could potentially be the hydrogen source for the H_2Bioil process. From previous model compounds studies conducted with the standalone fixed-bed reactor system studies (Task B.3 completed in FY11-Q4) Pt and Ru-based supported metal catalysts seem promising. Therefore, Task B.5 was completed with a 5%Pt/MWCNT (Multi-walled Carbon Nanotubes) catalyst to determine its performance in a H_2/CO gas mixture.

The H_2/CO co-feeding study was conducted on the lignin-derived model compound Dihydroeugneol ((DHE) 2-methoxy-4-propyl-phenol) at conditions of 300°C, ~24 bar total pressure, 0.08 bar DHE partial pressure, 0.45 bar Argon (used as an internal standard) partial pressure, and 0.9 hr^{-1} weight hourly space velocity (WHSV). Conditions with no CO co-feeding had a hydrogen partial pressure of 23.6 bar and conditions with CO co-feeding had a hydrogen partial pressure of 21.7 bar and a CO partial pressure of 1.9 bar. The catalyst underwent a reaction period of 24 hours before data was collected to ensure that the catalyst was stable.

Results of the CO co-feeding study can be found in Table 29. With no CO present, the 5%Pt/MWCNT had a conversion of 85% with the major product being the deoxygenated product 4-propyl-cyclohexanol. When CO was co-fed, the 5%Pt/MWCNT catalyst was poisoned and the conversion dropped to 1.5%.

Table 29. Conversion and product selectivity for the CO co-feeding study on a 5%Pt/MWCNT catalyst.

	5%Pt/MWCNT	
	No CO	**CO Co-feeding**
Partial Pressure of CO / bar	0	1.9
Partial Pressure of hydrogen/ bar	23.5	21.7
Conversion / %	**85**	**1.5**
	Selectivity / %	
HDO products		
Methane	2.3	13.5
Methanol	5.6	11.5
Benzene, propyl-	0.06	0.14
Phenol, 4-propyl-	3.6	32
Ring hydrogenation products		
Cyclohexane, propyl-	0.3	0.1
4-propylcyclohexanol	31.1	1
4-Propylcyclohexanone	3.7	0.4
2-methoxy-4-propyl cyclohexanol	31	1.4
Other Products	22.34	39.96

This study shows that the noble metal (Pt and Ru) based catalysts are not tolerant to large partial pressures of CO, and the catalyst activity is lost in H_2/CO mixtures. Based on this result of Task B.5 (catalyst testing and development of model compounds while introducing CO along with H_2), Task C.3 (biomass pyrolysis with catalysts in presence of CO/H_2) will not be conducted, as it is hypothesized that the noble metal (Pt and Ru) based catalysts used to complete Task C.2 will also be poisoned during a H_2/CO co-feeding studies.

If the integration of the H_2Bioil process with industrial processes such as methane reforming or coal power plants were to be successfully implemented in the future, further work on catalyst development would be needed to find catalysts that are at least as active and selective to hydrodeoxygenation as the Pt and Ru based catalysts, but that are also more resistant to CO poisoning.

Task number: [C] Biomass Sample Studies

In this section, we would like to point out that all grant tasks and milestones related to Task C involving real biomass fast-hydropyrolysis and hydrodeoxygenation catalysts testing have been completed. These results have been documented in the various quarterly reports associated with the grant. For instance, we achieved practical reactor performance milestones C.ML.1 (50% conversion to liquids and gases from biomass fast-hydropyrolysis and fast-pyrolysis) in the lab scale cyclone reactor using locally harvested sorghum as real biomass feedstock in FY11-Q2.
In addition to this, we performed fast-hydropyrolysis (FHP) on the sorghum feedstock (Task C.1) and hydrodeoxygenation (Task C.2) with candidate catalysts (identified from model compound studies) on sorghum FHP vapors which achieved up to 30% feed oxygen removal in the cyclone reactor and 100% deoxygenation to produce fully deoxygenated hydrocarbons in the micro-scale reactor. These results met the deoxygenation milestone C.ML.2 (35 wt% reduction of oxygen in oil made from a real biomass feedstock using high-pressure fast-hydropyrolysis with or without a HDO catalyst as compared to conventional pyrolysis in inert atmosphere). Again, we note that reaching 100% feed deoxygenation with biomass fast-hydropyrolysis vapors is inherently a very important milestone that took years of research and development to achieve.

Task number: [C.1] - Fast-hydropyrolysis in a single stage

High-Pressure, Continuous-Flow Fast-hydropyrolysis Reactor

In quarter FY11-Q2, we achieved milestone C.ML.1 (successful fast-pyrolysis of real biomass sample with a minimum 50% conversion of real biomass sample into liquids and gases in the pyrolysis reactor under inert atmosphere) by testing locally harvested sorghum feedstock in the lab-scale high-pressure fast-hydropyrolysis reactor. After initial experiments, improvements were implemented in the reactor design and heating scheme which helped in increasing time-on-stream for the high-pressure fast-pyrolysis of sorghum. In quarter FY11-Q4, we finished further experiments on high-pressure inert atmosphere fast-pyrolysis and comparative high-pressure fast-hydropyrolysis experiments with locally harvested sorghum as real biomass feedstock, which completed Task C.1.

The experiments were carried out on the high-pressure, cyclone-type, fast-hydropyrolysis reactor system, described in previous sections of this report. The feedstock for these experiments was locally harvested sorghum that was dried and milled to pass through a 40 mesh screen (< 420 µm). After pyrolysis, the vapor products passed through the catalytic fixed-bed reactor (with no catalyst for the base case experiments), and then to a condenser that cools the vapors to <20^{o}C. Condensed vapors were separated from permanent gases by a coalescing filter and the liquid products were collected in a trap. A sample of the exhaust gases was analyzed with a gas chromatograph (GC) with a thermal conductivity detector (TCD) to measure the

composition of carbon monoxide, carbon dioxide, and methane in the gas phase products. The collected liquid products (organics + water) were analyzed by Karl Fischer titration to determine the water content, which was used as a measure of the extent of hydrodeoxygenation in the experiments.

Table 30. Experimental conditions summary for fast-hydropyrolysis and fast-pyrolysis experiments with locally harvested sorghum feedstock.

	Fast-pyrolysis	*Fast-hydropyrolysis*
Feedstock	<420 µm sorghum	<420 µm sorghum
Feed rate / g min^{-1}	0.4	0.4
Total mass fed / g	29	22
Hydrogen flow rate / (std) L min^{-1}	0	7.6
Helium flow rate / (std) L min^{-1}	34.8	27.2
Nitrogen flow rate / (std) L min^{-1}	3.0	3.0
Total pressure / bar	26	26
Hydrogen partial pressure / bar	0	5
Helium partial pressure / bar	24	19
Nitrogen partial pressure / bar	2	2
Average pyrolysis temperature / °C	~535	~535
Vapor residence time in reactor / s	2.1	2.1

Table 30 shows the experimental conditions used for the fast-pyrolysis and comparative fast-hydropyrolysis experiments with sorghum. The pyrolysis temperature, total pressure and vapor residence times were comparable for both the experiments. The product yields from these experiments are shown in Figure 23. The liquid yield from the fast-hydropyrolysis experiment was higher than the fast-pyrolysis experiment, but the difference was not statistically significant, accounting for experimental error. The char yields of both the experiments were comparable but higher than that obtained from cellulose, at about ~23% due to the large particle size of sorghum, which reduced the heat transfer rate to the particles. The gas yields in both the experiments were comparable. Figure 24 shows that the gas phase composition of carbon monoxide, carbon dioxide and methane, which were comparable in both these experiments. Hence, there were no significant differences in the overall product distribution between high-pressure fast-pyrolysis and fast-hydropyrolysis of sorghum. This fast-hydropyrolysis experiment, with no HDO catalyst, was used as a baseline comparison for deoxygenation in the presence of candidate HDO catalysts in a high-pressure hydrogen environment (Task C.2).

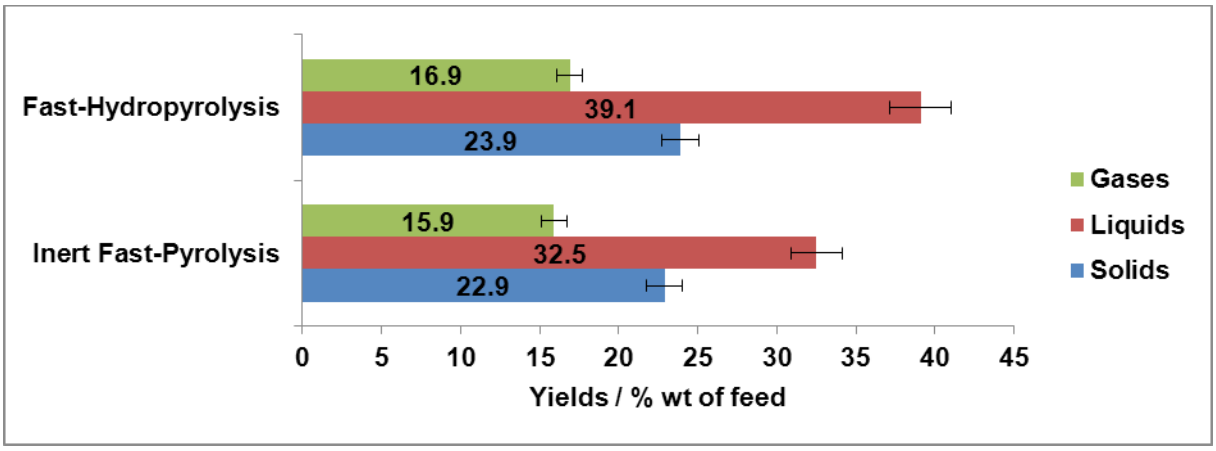

Figure 13. Liquids, solids and gaseous yields from the fast-pyrolysis and fast-hydropyrolysis of sorghum.

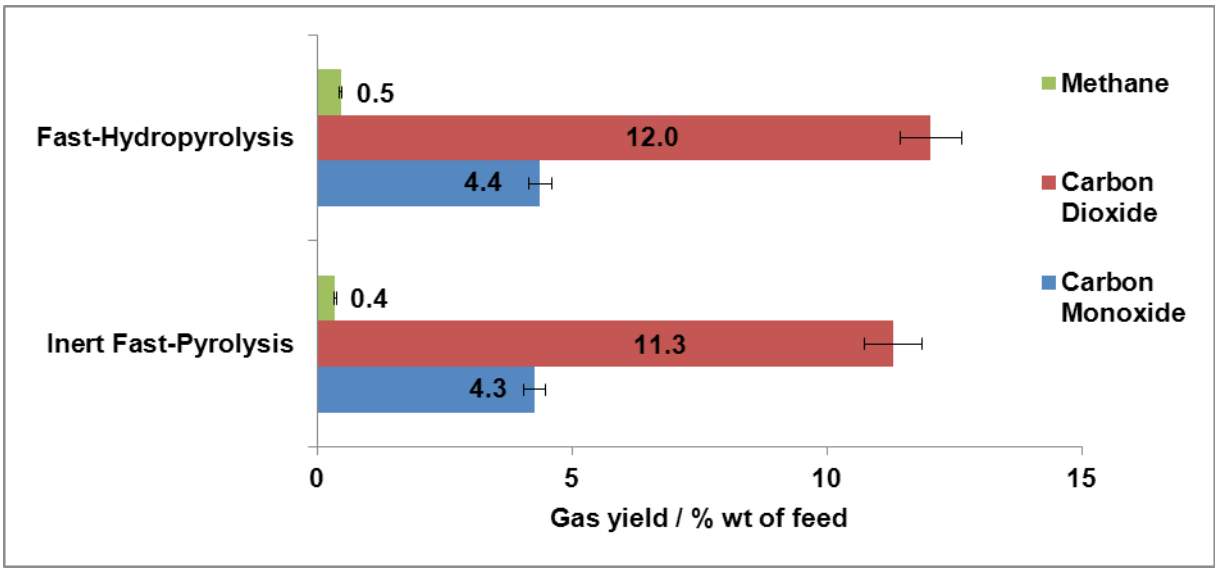

Figure 14. Composition of gaseous products produced from the fast-pyrolysis and fast-hydropyrolysis of sorghum.

Task number: [C.2] - Catalyst testing and development - I - biomass pyrolysis with catalysts

In FY-13 Q2, we completed experiments for Task C.2 using Ru-based and Pt-based candidate HDO catalysts, as identified from the standalone HDO reactor studies (as part of Task B.3) using model compounds, in both the lab-scale and micro-scale batch fast-hydropyrolysis reactors. Up to 30% feed oxygen removal in the cyclone reactor and 100% deoxygenation to produce fully deoxygenated hydrocarbons in the micro-scale reactor were achieved, meeting the deoxygenation milestone C.ML.2 (35 wt% reduction of oxygen in oil made from a real biomass feedstock using high-pressure fast-hydropyrolysis with or without a HDO catalyst as compared to conventional pyrolysis in inert atmosphere).

High-Pressure, Continuous-Flow Fast-hydropyrolysis Reactor

In this section, the candidate HDO catalyst experiments that were carried out on the high-pressure, cyclone-type, fast-hydropyrolysis reactor system, with locally harvested sorghum as the feedstock, are described. The catalysts used were a 2% Ru/Al_2O_3 (3.2 mm diameter trilobes from Alfa Aesar) and γ-Al_2O_3 (1.8mm diameter extrudates from Sasol). The Ru-based catalyst was reduced, *in situ*, at 375 ^oC in hydrogen before the experiment. For these experiments with sorghum, the experimental procedures were similar to the cellulose experiments reported in earlier sections of this report.

Table 31 shows the experimental conditions used for the sorghum fast-hydropyrolysis experiments with the two candidate HDO catalysts and comparative fast-hydropyrolysis experiment without a HDO catalyst. The hydropyrolysis temperature, hydrogen partial pressure, total pressure and residence times were comparable for all the experiments. The WHSV was lowered for the experiment with the Al_2O_3 catalyst in an attempt to improve extent of deoxygenation to meet the C.ML.2 oxygen reduction milestone. The product yields from these experiments are shown in Table 32. The elemental analyses and the water content of the liquid products from the experiments are shown in Table 33.

Table 31. Experimental conditions summary for sorghum fast-hydropyrolysis experiments with 2%Ru/Al_2O_3 and Al_2O_3 as HDO catalysts and comparative experiment without a HDO catalyst.

	Fast-hydropyrolysis with 2%Ru/Al_2O_3 as HDO catalyst	*Fast-hydropyrolysis with Al_2O_3 as HDO catalyst*	*Fast-hydropyrolysis without HDO catalyst (for comparison)*
Feedstock	Sorghum < 40 mesh	Sorghum < 40 mesh	Sorghum <40 mesh
Biomass feed rate / g min^{-1}	0.4	0.5	0.4
Total biomass fed / g	24.0	37.0	22.3
Hydrogen flow rate / (std) L min^{-1}	7.6	7.6	7.6
Helium flow rate / (std) L min^{-1}	27.2	27.2	27.2
Nitrogen flow rate / (std) L min^{-1}	3.0	3.0	3.0
Total pressure / bar	26	26	26
Hydrogen partial pressure / bar	5	5	5
Helium partial pressure / bar	19	19	19
Nitrogen partial pressure / bar	2	2	2
Average pyrolysis temperature / °C	~535	~535	~535
Vapor residence time in reactor / s	2.1	2.1	2.1
HDO catalyst	*2% Ru/Al_2O_3*	*Al_2O_3*	-
Weight hourly space velocity / hr^{-1}	4.5	3.0	-
Average catalyst bed temperature / °C	~375	~375	-

Table 32. Overall mass balance for fast-hydropyrolysis experiments with and without HDO catalyst (for comparison) for sorghum as real model feedstock.

	Fast-hydropyrolysis with 2%Ru/Al_2O_3 as HDO catalyst	*Fast-hydropyrolysis with Al_2O_3 as HDO catalyst*	*Fast-hydropyrolysis without HDO catalyst (for comparison)*
Liquid yield / wt %	33.8	37.7	39.1
Char + coke yield / wt %	26.8	30.5	23.9
Gas yield / wt %	16.1	18.0	16.9
CO / wt %	4.3	4.6	4.4
CO_2 / wt %	7.3	12.7	12.0
CH_4 / wt %	4.5	0.5	0.5
C_2H_4 / wt %	0.6	0.3	0
Overall Mass Balance	77	86	80

Table 33. Elemental analysis of liquid products produced from fast-hydropyrolysis experiments with and without HDO catalyst (for comparison) for sorghum (Empirical formula $CH_{1.806}N_{0.006}O_{0.845}$) as a real biomass feedstock.

	Fast-hydropyrolysis with 2%Ru/Al_2O_3 as HDO catalyst	*Fast-hydropyrolysis with Al_2O_3 as HDO catalyst*	*Fast-hydropyrolysis without HDO catalyst (for comparison)*
Carbon (wet basis) / wt %	10.6	14.3	17.0
Hydrogen (wet basis) / wt %	9.9	10.9	9.3
Oxygen (wet basis) by difference / wt %	0.5	73.5	73.2
Water content / wt %	80.3	72.4	65.2
Carbon (dry basis) / wt %	53.6	51.8	48.8
Hydrogen (dry basis) / wt %	4.4	10.0	5.7
Nitrogen (dry basis) / wt %	2.7	4.6	1.1
Oxygen (dry basis) by difference / wt %	39.2	33.5	38.1
Empirical formula (dry basis)	$CH_{0.97}N_{0.044}O_{0.55}$	$CH_{2.3}N_{0.077}O_{0.49}$	$CH_{1.39}N_{0.025}O_{0.68}$
% weight reduction in oxygen in liquid (dry basis) as compared to feed	17.6	29.6	7.5

In the presence of the 2%Ru/Al_2O_3 catalyst the liquid yield was lower as compared to the fast-hydropyrolysis experiment without a HDO catalyst. This was due to the higher yields of CH_4 with the 2%Ru/Al_2O_3 catalyst, signifying methanation, similar to the results with cellulose as a model biomass feedstock. The extent of deoxygenation was about ~18% as compared to ~8% without a HDO catalyst.

In the presence of the Al_2O_3 catalyst, the liquid yield was again lower as compared to the fast-hydropyrolysis experiment without a HDO catalyst. This was due to coking on the Al_2O_3 surface in the absence of a metal function, similar to the results with cellulose as model biomass feedstock. The water content of the liquid product in the presence of Al_2O_3 was higher than the comparative experiment without a HDO catalyst, which signified dehydration on the acid catalyst. The lower WHSV of ~3 hr^{-1} in Al_2O_3 experiment led to a higher extent of deoxygenation of ~30% as compared to ~18% with 2% Ru/Al_2O_3 at a WHSV of 4.5 hr^{-1}. This shows that a further reduction in the WHSV (with higher catalyst-to-feed rate ratios) could improve the extent of deoxygenation to ≥35% to meet the C.ML.2 oxygen reduction milestone.

In summary, high-pressure fast-hydropyrolysis experiments, with candidate HDO catalyst 2%Ru/Al_2O_3 and Al_2O_3 as an acid catalyst were completed with locally harvested sorghum as a real biomass feedstock. These experiments completed Task C.2. Similar to the results with cellulose, the 2%Ru/Al_2O_3 catalyst favored methanation and Al_2O_3 favored dehydration. The Al_2O_3 catalyst coked due to the absence of a metal, whereas there was no coking on the 2% Ru/Al_2O_3 catalyst due to the presence of the Ru

metal function. The extents of deoxygenation improved from ~18% in the presence of the 2% Ru/Al_2O_3 catalyst to ~30% with Al_2O_3 catalyst by the reduction of WHSV. These experiments showed that further reduction in WHSV (or higher catalyst-to-feed rate ratios) could improve the extent of deoxygenation to meet the C.ML.2 oxygen reduction milestone. Hence, bookend WHSV experiments, with excess catalyst-to-feed ratios of ~20, were carried out on the micro-batch fast-hydropyrolysis reactor with sorghum as a real biomass feedstock, as explained in the next section of the report.

Micro-batch, Fast-hydropyrolysis Reactor

In FY13-Q2, the micro-batch fast-hydropyrolysis reactor was used for studying the upgrading of hydropyrolysis vapors over a $2\%Pt/ZrO_2$ catalyst, using sorghum as a real biomass feedstock, in conjunction with the high-pressure lab-scale fast-hydropyrolysis reactor as part of task C.2. The $2\%Pt/ZrO_2$ catalyst was chosen over the $2\%Ru/ZrO_2$ catalyst due to results of better selectivity towards C_4+ hydrocarbons with cellulose as model feedstock. All the experimental conditions were similar to that of cellulose upgrading, as described earlier in this report, and the catalyst-to-feed ratio was 19. The product distribution (Tables 34 and 35) of upgraded products from sorghum was different from the experiment on upgrading of cellulose hydropyrolysis products, due to presence of hydropyrolysis products from the lignin and the hemicellulose fraction of the real biomass. Significant amounts of C_8 products were observed with sorghum, with the major C_8 product being ethyl cyclohexane. The cyclic structure of this compound indicates that it was a product of the lignin fraction of the biomass and its absence from the cellulose upgrading products supports this hypothesis.

Table 34. Products observed during upgrading of sorghum hydropyrolysis vapors over $2\%Pt/ZrO_2$ catalyst.

Groups	Products
C_1	CO,Methane
C_2	Ethane
C_3	Propane
C_4	Butane, Isobutane
C_5	Cyclopentane, 2-Methylbutane, n-Pentane
C_6	Methylcyclopentane, Cyclohexane, 2-Methylpentane, Hexane
C_7	Methylcyclohexane, Ethylcyclopentane, 3-Methylhexane, Heptane
C_8	Ethyl cyclohexane, Octane

Table 35. Product distribution represented as carbon percentage with respect to the total carbon in the biomass. Product distribution upgrading of sorghum hydropyrolysis vapors in the micro-batch fast-hydropyrolysis reactor over a 2%Pt/ZrO_2 catalyst (23mg) at H_2 partial pressure of 25 bar and temperature of catalyst bed at 300°C.

Catalyst	**2%Pt/ZrO_2**
CO	2.9
CH_4	10.3
C_2	8.8
C_3	5.2
C_4	5.3
C_5	7.2
C_6	6.7
C_7	4.3
C_8	5.1
Others	4.9
Char*	34.3
Total	95.2

* assumption – 70% of the char is composed of carbon.

Similar to cellulose fast-hydropyrolysis experiments, the sorghum fast-hydropyrolysis experiments in the micro-batch fast-hydropyrolysis reactor, with the candidate HDO catalyst 2%Pt/ZrO_2, have shown that it is possible to achieve 100% deoxygenation of biomass fast-hydropyrolysis vapors, using a high catalyst-to-feed ratio of 19. These experiments have met the C.ML.2 milestone (minimum 35% weight reduction of oxygen in oil made from a real biomass feedstock using high pressure fast-hydropyrolysis with or without a HDO catalyst as compared to conventional pyrolysis in inert atmosphere). These experiments have shown that it would be possible to achieve greater extents of deoxygenation in the lab-scale continuous reactor by moving to lower WHSV (or higher catalyst-to-feed rate ratios).

Task C.1 was completed with successful demonstration of fast-hydropyrolysis of sorghum in the lab-scale continuous reactor. The effect of presence of hydrogen during pyrolysis of biomass was studied and no significant change in product distribution was observed. Presence of catalysts along with high partial pressure of hydrogen is the key for deoxygenation of pyrolysis products to fuel range molecules. Task C.2 was completed with the micro-scale batch reactor with 100% deoxygenation of pyrolysis products from sorghum. All the milestones were completed with successful demonstration of > 35% weight reduction of oxygen in oil made from a real biomass feedstock. These results along with results from Task B.2, demonstrate significant development in catalysts for hydrodeoxygenation of pyrolysis products from biomass. No further development is needed as a part of this project, with successful demonstration of production of fuel range molecules (C4+ hydrocarbons) from real biomass feedstock.

Task number: [C.3] - Catalyst testing and development-II - biomass pyrolysis with catalysts in presence of CO/H_2

Studies as part of Task B.5 (catalyst testing and development of model compounds while introducing CO along with H_2), showed that the noble metal (Pt and Ru) based catalysts are not tolerant to large partial pressures of CO, and the catalyst activity is lost in H_2/CO mixtures. Hence, Task C.3 (biomass pyrolysis with catalysts in presence of CO/H_2) was not conducted, as it is hypothesized that the noble metal (Pt and Ru) based catalysts used to complete Task C.2 will also be poisoned during H_2/CO co-feeding studies.

Task number: [D] Demonstration plan for H_2Bioil-I process

In lieu of a demonstration plan (Task D) and revisions of earlier process modeling (Task E), the major findings from the experimental and modeling activities of the project were reported in the quarterly report of Q-2 FY13. In that document, the challenges that remain to be addressed in the experimental demonstration of the H_2Bioil-I process were also discussed. This information will be useful for any future activities concerned with building a demonstration unit of the H_2Bioil-I process.

Task number: [E] Continue systems analysis

Activities under Task E of this project have focused on using energy systems analysis tools to identify carbon and energy efficient processes for harnessing solar energy to meet various energy demands, such as transportation fuels. Particular emphasis was given to identifying new ideas to guide the development of biofuel processes that maximize energy efficiency and minimize resource requirements. For this task of the project, the following two milestones were achieved at the end of Q-4 FY-11.

- Develop processes that maximize biomass carbon conversion to liquid fuel while using the least supplemental (solar) energy input (E.M.L 1).
- Identify a renewable technology portfolio capable of meeting a percentage of the current US transportation demand while minimizing the primary energy used (E.M.L 2).

Description of the main results

Synthesis of augmented biofuel processes

A major research thrust of this task has been the identification of energy and carbon efficient biomass-to-liquid fuel (biofuel) processes to meet the energy demands of the transportation sector. In particular, we have focused on modeling augmented biofuel processes, which utilize supplementary solar energy in the form of heat, H_2 or electricity to recover a greater fraction of biomass carbon atoms as liquid fuel.

During the first two years of the project (FY09-1 to FY09-4 and FY10-1 to FY10-4), we used simulation tools like Aspen Plus to investigate the following biomass thermochemical conversion routes: 1) gasification followed by Fischer-Tropsch (FT) and 2) fast-hydropyrolysis followed by catalytic hydrodeoxygenation (HDO). For example, we modeled the solar thermal biomass gasification (STG) process, involving high temperature (~1400 K) biomass steam gasification using solar heat followed by Fischer-Tropsch (FT) synthesis. In addition to an increase in the estimated biofuel yield compared to conventional gasification/FT processes (12.8 vs 8.6 MJ of fuel/kg of biomass), the STG process offers a means of storing additional solar energy in an easy-to-use form, by upgrading the calorific value of the biomass feedstock. Similarly, we modeled an augmented process based on the use of solar heat in conjunction with biomass fast-hydropyrolysis/HDO (referred as H_2Bioil-STG), with an estimated yield of 12.3 MJ of fuel/ kg of biomass corresponding to 49.7% carbon recovery (η_{carbon}) as liquid fuel. Here, the H_2 needed for fast-hydropyrolysis/HDO originates from the syngas produced by gasifying a portion of the feed biomass using solar heat.

Although useful for initial screening, simulation-based analyses are limited in their ability to identify the limits of process performance as well as heat and mass integration opportunities. With this in mind, we developed a systematic process synthesis approach whereby different process designs can be simultaneously evaluated. We formulated a mixed integer nonlinear programming (MINLP) model that allows for simultaneous mass, heat, and power integration over a derived process superstructure. Figure 25 is

an example superstructure based on the aforementioned thermochemical routes that was investigated. The models used to mathematically describe biomass fast-hydropyrolysis/HDO were derived from the experimental information published by the Gas Technology Institute (GTI) from their pilot plant studies with woody biomass (1).

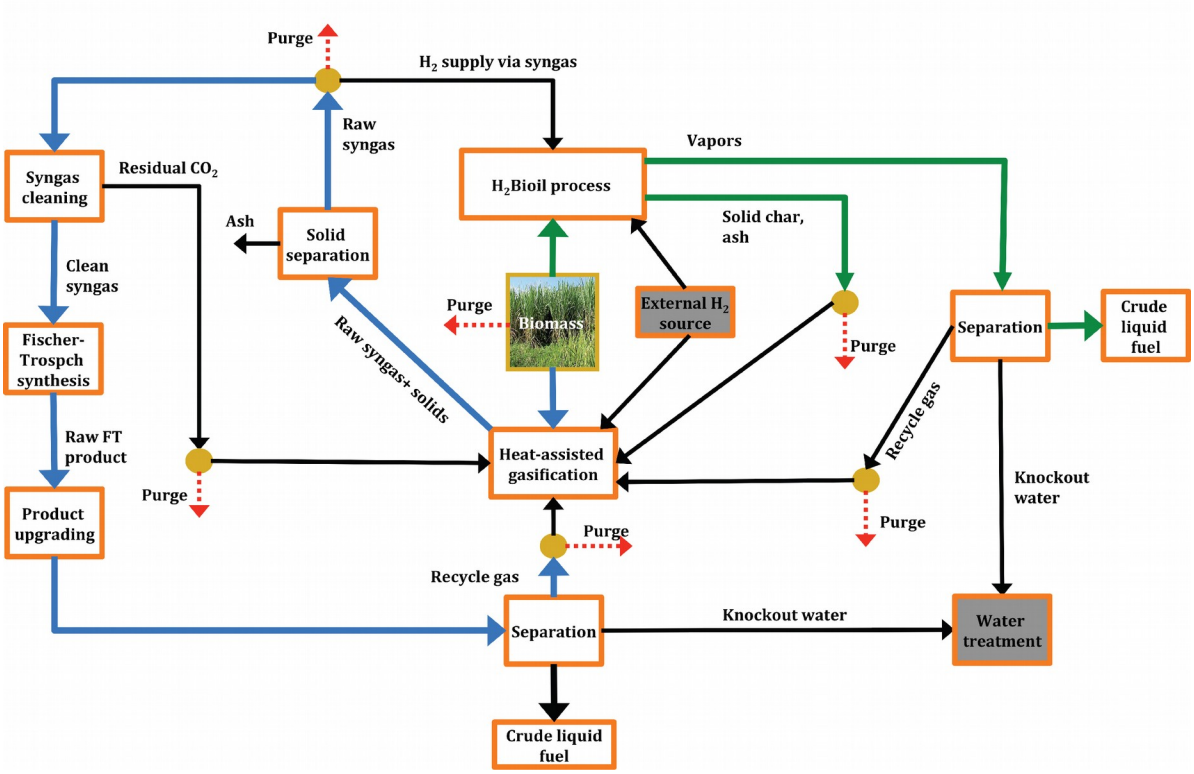

Figure 15: Simplified representation of the process superstructure combining biomass gasification-FT (marked in blue) and fast-hydropyrolysis/HDO pathways (marked in green). All the purge streams (dotted red) are utilized for their heating value via combustion. The shaded units have not been modeled.

For every target value of carbon recovery as liquid fuel (η_{carbon}), the solution of the MINLP model, obtained using global optimization tools (2), identified the biofuel process configuration requiring the least solar energy input as heat, electricity, and H_2. As shown in Figure 26, the optimal configuration identified using the developed MINLP model can be categorized either as standalone ($\eta_{carbon} \leq 54\%$), augmented using solar heat ($55 \leq \eta_{carbon} \leq 74\%$) or augmented using solar heat and H_2 ($74\% \leq \eta_{carbon} \leq 95\%$). Importantly, the H_2 consumption of the augmented process configurations is found to be close to the derived theoretical minimum values, as seen in Figure 26. The synergistic gain of the proposed thermochemical process integration is evidenced from the ~28-156% lower estimated solar energy consumption compared to gasification/FT processes, for η_{carbon} between 70% and 95%.

To address the intermittency of solar energy availability, we also identified robust biofuel process designs that are capable of operating either in standalone (low η_{carbon}) or augmented (high η_{carbon}) process modes. If this flexibility in process carbon recovery can be attained without startup and shutdown of units, then the process can be operated

continuously even if cost-effective solar energy storage methods are not available. Alternatively, the identified augmented biofuel processes can operate round the clock by integrating with renewable energy storage systems. In a transition scenario, coal and natural gas can supplement biomass during times of solar energy unavailability.

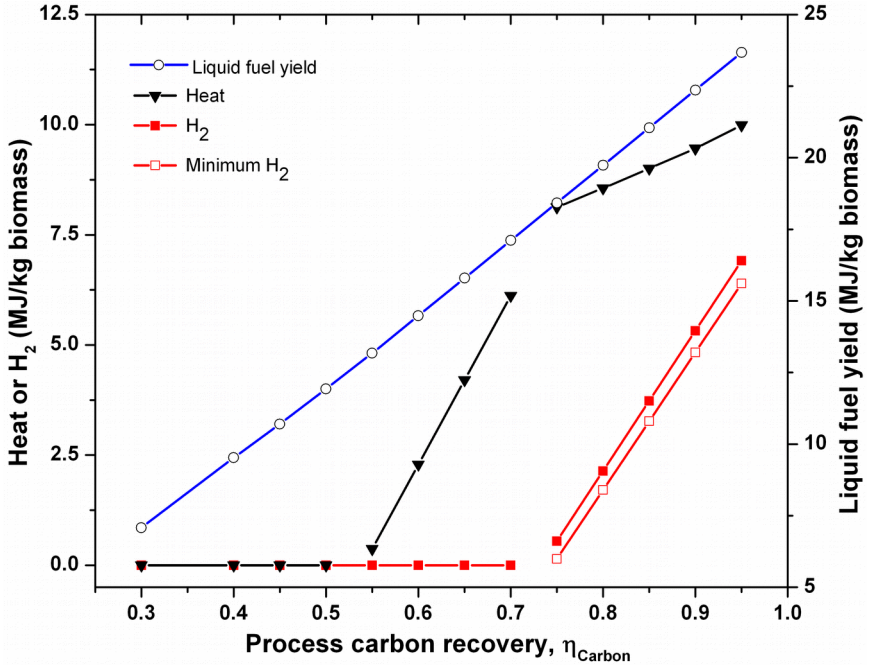

Figure 16. Solar heat, H_2 consumption and liquid fuel yield of the optimal process configuration for different target carbon recovery levels. FT product distribution as per Anderson-Schulz-Flory product distribution (3); fast-hydropyrolysis/HDO biomass carbon recovery in liquid = 48% (1).

Biomass vs other routes for liquid fuel

In case liquid fuel produced from sustainably available biomass is insufficient to meet the liquid fuel needs of the transportation sector, additional carbon and land resources must be allocated for this end use (4). For such a case, we investigated alternative routes for converting atmospheric CO_2 to liquid fuel using solar energy in FY10-2 and FY10-3. The analysis relied on the metric of sun-to-fuel (STF) efficiency, referring to the fraction of incident solar energy that is recovered in the liquid fuel.

We investigated the conversion of a concentrated CO_2 stream recovered from air to liquid fuel via a feasible thermochemical route based on high temperature reverse water-gas shift reaction followed by FT synthesis. The overall process energy inputs include hydrogen, high temperature heat and electricity produced from solar energy. Using currently available technologies, the likely STF efficiency of this CO_2 extraction/thermochemical route was estimated to be 4.06 %. This is higher than the current STF efficiency estimate of 0.96% for the photosynthetic route of growing biomass followed by augmented biofuel production (4). The direct use of algal oil and conversion of the residue via a thermochemical route to liquid fuel was estimated to

have STF efficiency values for current and potential future algae yields of 1.82 % and 3.68 % respectively. Therefore, in a renewable economy setting with limited land available for harnessing solar energy, CO_2 extraction from the air followed by thermochemical conversion was found to be the most efficient at storing solar energy as liquid fuel.

Economic/life cycle analysis

As an extension of the earlier modeling results, we also carried out an economic analysis for the proposed biomass fast-hydropyrolysis/HDO (H_2Bioil) process relying on hydrogen derived different primary energy sources (5). The break-even crude oil price for a delivered biomass cost of $94/metric ton when hydrogen is derived from coal, natural gas or nuclear energy ranges from $103 to $116/bbl for no carbon tax scenarios. This break-even crude oil price compares favorably with the literature estimated prices of fuels from alternative biofuel production routes. Among the different options, the H_2Bioil process using hydrogen from natural gas is particularly interesting, given the recent expansion in US natural gas reserves.

The economic analysis also revealed much higher break-even crude oil prices when using hydrogen from renewable energy sources like wind ($139/bbl) and solar energy ($219/bbl). However, it should be noted that the technologies relevant to harnessing renewable energy (e.g. solar hydrogen production) are at an early stage of development. Therefore, current economic parameters (capital cost, operating costs etc.) for these technologies are often poor indicators of their future cost.

Conclusion and impact

The systems analysis efforts have identified carbon and energy efficient biomass-to-liquid fuel process designs that integrate the use of different primary energy sources along with biomass (e.g. solar, coal or natural gas) for liquid fuel production. In particular, we identified augmented biomass-to-liquid fuel configurations based on the fast-hydropyrolysis/HDO pathway, which is being experimentally studied under Tasks B and C of this project. With these developments, this task has conditionally met the E.ML.1 & E.ML.2 milestone metrics of identifying process configurations capable of producing 6.2 Million barrels (MMbl) d^{-1} of transportation fuels while maximizing biomass carbon usage along with using the minimum solar energy input to meet 50% of the current US transportation fuel demand. It should also be pointed out that the computational tool developed for screening alternative process configurations represents a unique contribution to the field of biomass processing for liquid fuel production.

Based on the findings of task, we have also engaged outside groups, including GTI. Our presentation of technology and modeling results to GTI resulted in their developing a pilot scale process. The pilot plant from GTI is proof that our proposed process is currently the only commercially available process for high energy density liquid fuel production in one single step from entire biomass constituents. Further, an economic

analysis of the H_2Bioil process revealed that the break-even crude oil price compares favorably with the literature estimated prices of fuels from alternate biochemical and thermochemical routes, suggesting that the development of H_2Bioil process must be pursued vigorously.

References

1. Marker TL, et al. 2012. Integrated Hydropyrolysis and Hydroconversion (IH2) for the Direct Production of Gasoline and Diesel Fuels or Blending Components from Biomass, Part 1: Proof of Principle Testing, *Environmental Progress & Sustainable Energy* 31: 191-199
2. Tawarmalani, M. and Sahinidis, N. V. 2005. A polyhedral branch-and-cut approach to global optimization. *Mathematical Programming* 103:225-249.
3. Dry, M. E. 2002. The Fischer-Tropsch process: 1950-2000. *Catalysis Today* 71: 227-241.
4. Mallapragada, D. S., Singh, N. R., Curteanu, V., Agrawal, R. 2013. Sun-to-Fuel Assessment of Routes for Fixing CO2 as Liquid Fuel. *Industrial & Engineering Chemistry Research* 52: 5136-5144.
5. Singh, N., Mallapragada, D., Agrawal, R., Tyner, W. 2012. Economic analysis of novel synergistic biofuel (H2Bioil) processes. *Biomass Conversion and Biorefinery* 2:141-148.

Patents:

1. *Integrated Gasification-Pyrolysis Process*, R. Agrawal and N. R. Singh, US Patent#8,217,210 B2, (2012).

2. P*rocess for Producing Liquid Hydrocarbon by Pyrolysis of Biomass in Presence of Hydrogen from a Carbon-free Energy Source*, R. Agrawal, M. Agrawal and N. R. Singh, US Patent#8,217,211 B2, (2012).

Publications / Presentations:

1. Agrawal R., Singh N.R., ”Synergistic Routes to Liquid Fuel for a Petroleum Deprived Future”, AIChE J 55 7 2009 p1898-1905.

2. Agrawal, R., Singh, N.R., Ribeiro, F.H., Delgass, W.N., Perkis, D.F., Tyner, W.E., ”Synergy in the hybrid thermochemical–biological processes for liquid fuel production”, Computers and Chemical Engineering 33 12 2009 p2012-2017.

3. Singh, N.R., Delgass, W.N., Ribeiro, F.H., Agrawal, R., “Estimation of Liquid Fuel Yields from Biomass”, Environmental Science and Technology 44 13 2010 p5298-5305

4. Agrawal, R., Singh, N.R., “Solar Energy to Biofuels”, Review of Chemical and Biomolecular Engineering 11 2010 p343-364

5. Agrawal, R., Mallapragada, D.S., “Chemical Engineering in a Solar Energy Driven Sustainable Future”, AIChE J 56 11 2010 p2762-2768.

6. Mallapragada D. S., Singh, N.R., Agrawal, R., “Energy Systems Analysis for a Renewable Transportation Sector”, in 21st European Symposium on Computer Aided Process Engineering-ESCAPE 21, eds. E. N. Pistikopoulos, M. C. Georgiadis and A. Kokossis, Elsevier B.V, Chalkidiki, Greece, 2011.

7. Mallapragada,D.S., Singh, N.R., Curteanu, V., Agrawal, R., Sun-to-Fuel Assessment of Routes for Fixing CO_2 as Liquid Fuel, Ind Eng Chem Res 52 14 2013 p5136-5144.

8. Singh, N.R., Ribeiro, F.H., Delgass, W.N., Agrawal, R., Synergistic Use of Solar Hydrogen with Biomass to Produce Biofuels, American Institute of Chemical Engineers National Meeting, 2008, Philadelphia, PA.

9. Agrawal, R., Transportation Fuel in a Solar Economy, Foundations of Computer-Aided Process Design Meeting, 2009, Breckenridge, CO

10. Singh, N.R., Agrawal, R., Synergistic Routes to Liquid Fuel for a Petroleum Deprived Future, American Institute of Chemical Engineers National Meeting, 2009, Nashville, TN

11. Singh, N.R., Agrawal, R., Synergistic Routes to Liquid Fuel for a Petroleum Deprived Future, American Institute of Chemical Engineers National Meeting, 2009, Nashville, TN

12. *Sara L. Yohe, W. Nicholas Delgass, Fabio H. Ribeiro, Rakesh Agrawal*, *High Pressure Catalytic Hydrodeoxygenation of Hydro-pyrolysis Vapor Lignin Model Compounds*, American Institute of Chemical Engineers National Meeting, 2011, *Minneapolis, MN*

13. *Vinod Kumar Venkatakrishnan, Andrew D. Smeltz, Sergey V. Semikolenov, Fabio H. Ribeiro, W. Nicholas Delgass and Rakesh Agrawal*, High Pressure Fast-Pyrolysis and Fast-Hydropyrolysis for Conversion of Biomass to Liquid Fuels, American Institute of Chemical Engineers National Meeting, 2011, *Minneapolis, MN*

14. Singh, N. R., Mallapragada D., Agrawal R., Tyner W. E., “Economic analysis of novel synergistic biofuel (H_2Bioil) processes”, Biomass Conv. Bioref. 2 2012 p141-148

15. *Sara L. Yohe, W. Nicholas Delgass, Fabio H. Ribeiro, Rakesh Agrawal*, Kinetics of *High Pressure Catalytic Reaction Pathways for Dihydroeugenol of Pt/ZrO2*, American Institute of Chemical Engineers National Meeting, 2012, *Pittsburgh, PA*

16. *Sara L. Yohe, W. Nicholas Delgass, Fabio H. Ribeiro, Rakesh Agrawal*, *High Pressure Catalytic Reaction Pathways and Kinetics of the Lignin Model Compound Dihydroeugenol over 2%Pt/ZrO_2,* 23rd North American Catalysis Society Meeting, 2013, *Louisville, KY*